Accepted for publication in ***Building and Environment*** (October 17, 2012)

Rainwater runoff from building facades: a review

B. Blocken* [(a)], D. Derome [(b)], J. Carmeliet [(b,c)]

(a) Building Physics and Services, Eindhoven University of Technology, P.O. box 513, 5600 MB Eindhoven, The Netherlands
(b) Laboratory for Building Science and Technologies, Swiss Federal Laboratories for Materials Testing and Research, Empa, Überlandstrasse 129, CH-8600 Dübendorf, Switzerland
(c) Chair of Building Physics, Swiss Federal Institute of Technology ETHZ, ETH-Hönggerberg, CH-8093 Zürich, Switzerland

Graphical abstract:

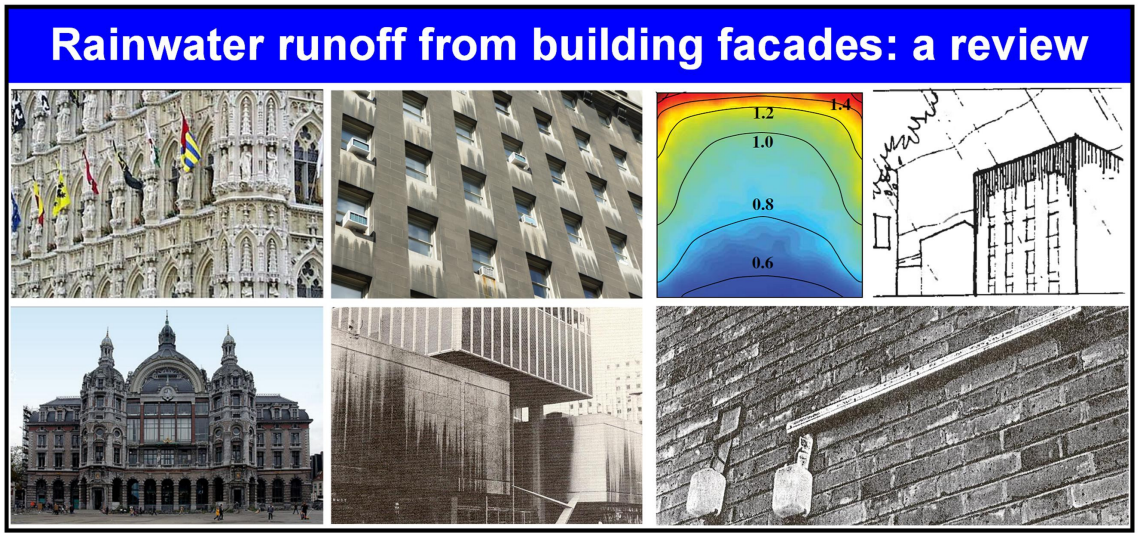

Research highlights:

- Rainwater runoff is responsible for rain penetration, surface soiling, biocide leaching, etc.
- Extensive review of rainwater runoff research by observations, measurements and modelling
- Review is based on knowledge of wind-driven rain impingement patterns and wind-blocking effect
- Review contains 239 papers, reports and books, mainly from the past 5 decades
- Information for future research, building design and improvement of hygrothermal models

* **Corresponding author**: Bert Blocken, Building Physics and Services, Eindhoven University of Technology, P.O.Box 513, 5600 MB Eindhoven, the Netherlands. Tel.: +31 (0)40 247 2138, Fax +31 (0)40 243 8595
E-mail address: b.j.e.blocken@tue.nl

Accepted for publication in ***Building and Environment*** (October 17, 2012)

Rainwater runoff from building facades: a review

B. Blocken* [(a)], D. Derome [(b)], J. Carmeliet [(b,c)]

(a) Building Physics and Services, Eindhoven University of Technology, P.O. box 513, 5600 MB Eindhoven, The Netherlands
(b) Laboratory for Building Science and Technologies, Swiss Federal Laboratories for Materials Testing and Research, Empa, Überlandstrasse 129, CH-8600 Dübendorf, Switzerland
(c) Chair of Building Physics, Swiss Federal Institute of Technology ETHZ, ETH-Hönggerberg, CH-8093 Zürich, Switzerland

Abstract
Rainwater runoff from building facades is a complex process governed by a wide range of urban, building, material and meteorological parameters. Given this complexity and the wide range of influencing parameters, it is not surprising that despite research efforts spanning over almost a century, wind-driven rain and rainwater runoff are still very active research subjects. Accurate knowledge of rainwater runoff is important for hygrothermal and durability analyses of building facades, assessment of indirect evaporative cooling by water films on facades to mitigate outdoor and indoor overheating, assessment of the self-cleaning action of facade surface coatings and leaching of particles from surface coatings that enter the water cycle as hazardous pollutants. Research on rainwater runoff is performed by field observations, field measurements, laboratory measurements and analytical and numerical modelling. While field observations are many, up to now, field experiments and modelling efforts are few and have been almost exclusively performed for plain facades without facade details. Field observations, often based on a posteriori investigation of the reasons for differential surface soiling, are important because they have provided and continue to provide very valuable qualitative information on runoff, which is very difficult to obtain in any other way. Quantitative measurements are increasing, but are still very limited in relation to the wide range of influencing parameters. To the knowledge of the authors, current state-of-the-art hygrothermal models do not yet contain runoff models. The development, validation and implementation of such models into hygrothermal models is required to supplement observational and experimental research efforts.

Keywords: Wind-driven rain; driving rain; wind flow; facade surface soiling; runoff leaching; urban heat island

1. Introduction

1.1. Wind-driven rain and related building pathology

> *"All buildings, whatever shortcomings they may have, are required to possess two fundamental characteristics. They should be structurally sound and they should exclude moisture." (Marsh 1977 [1])*

The co-occurrence of wind and rain causes wind-driven rain (WDR). WDR or driving rain is rain that is given a horizontal velocity component by the wind, that falls obliquely and that is driven against the windward facade of buildings. WDR is one of the most important moisture sources affecting the hygrothermal performance and durability of building facades [1-5]. Consequences of its destructive properties can take many forms. Moisture accumulation in porous materials can lead to rain penetration [1,3,6-17], frost damage [3,4,17-20], moisture-induced salt migration [4,17,18] discolouration by efflorescence [3,4,17], biological and chemical degradation of the building material and building components [21-34] and structural cracking due to thermal and moisture gradients [17], to mention just a few. When rain penetration occurs, WDR also becomes a moisture source for the building interior, possibly damaging interior surfaces and furniture (e.g. cultural heritage in historical buildings).

The problem of rain penetration can occur in masonry load bearing walls and cavity walls (also referred to as veneer-clad walls) as well as in curtain wall systems. Matthews et al. [35] state that about half of 1980s era e curtain wall buildings suffered leaks and that one third deteriorated unacceptably before the end of their design

* **Corresponding author**: Bert Blocken, Building Physics and Services, Eindhoven University of Technology, P.O.Box 513, 5600 MB Eindhoven, the Netherlands. Tel.: +31 (0)40 247 2138, Fax +31 (0)40 243 8595
E-mail address: b.j.e.blocken@tue.nl

life. These failures have required costly repairs and in 1991, an entire building had to be reclad [36]. Apart from rain penetration, WDR impact and runoff is also responsible for the appearance of surface-soiling patterns on facades, which have become characteristic for so many of our buildings [5,17,21,25,37-50]. As an example, Figure 1 displays the facade of the Royal Festival Hall in London, before and after a few years of exposure to atmospheric pollution and WDR. Although these issues have been widely and for a long time recognised as major building problems, damage claims and huge repair and replacement costs are still on the rise [5,36,51]. Three reasons are feeding the persistence of these problems. First, there is the increasing use of innovative design features, building technologies and materials in present-day construction, knowledge on the hygrothermal performance of which has not yet been fully attained. Second, the designs of many modern architects do not shed water from their facades in the way that pre-modern era buildings have done for centuries. Instead, in their strive for plane and smooth building facades with a minimum of details, many modern architects tend to abandon adequate facade detailing with cornices, ornated sills, parapets etc, which is essential for protection against WDR and rainwater runoff. Third, unlike most requirements of buildings where the design data can be expressed in quantitative terms, appropriate quantitative design data for WDR and rainwater runoff are lacking.

WDR and rainwater runoff are also important as part of indirect evaporative cooling by water films on exterior building surfaces that can reduce the required cooling load for the indoor environment and mitigate indoor and outdoor heat stress and the urban heat island effect [52-54]. WDR and runoff also contribute to the self-cleaning action of facade surface coatings and glass surface coatings [55,56]. On the other hand, the development and application of these coatings has also incited serious concerns about the leaching of (nano-)particles by WDR and rainwater runoff, by which these particles enter the water cycle as hazardous pollutants [57-60].

Knowledge on WDR and rainwater runoff is essential for the adequate design of building facades. WDR and rainwater runoff are essential boundary conditions for the study of the hygrothermal performance and durability of building facades with Heat-Air-Moisture (HAM) transfer models, for the analysis of indirect evaporative cooling and for the assessment of the self-cleaning action and leaching of facade surface coatings.

1.2. The two parts in wind-driven rain research

> *"But the question how to design our buildings so that no rain will penetrate can only be answered if the amount of water we have to resist is known." (Vos 1974 [61])*

The study of WDR in building research and building physics consists of two parts: (1) assessment of the impinging WDR on vertical building walls (before raindrop impact) and (2) assessment of the response of the building walls to the impinging rain (after raindrop impact) (Fig. 2). The first part of WDR research comprises the study of the movement and distribution of raindrops as they fall from the clouds and are carried by the wind in the atmospheric boundary layer until they impinge on the building facade. The impinging WDR intensity is governed by a wide range of parameters: urban geometry, building geometry, facade geometry, facade detailing, position on the building facade, and all relevant meteorological parameters such as wind speed, wind direction, rainfall intensity and raindrop-size distribution. The complex interaction of these parameters yields distinct WDR patterns across facades [5,17,38-41,46-50,62-109]. The second part of WDR research consists of the micro-scale physical processes that occur at and after impact of WDR at the building facade. It includes surface phenomena such as splashing, bouncing, adhesion, spreading and absorption of raindrops, film forming, runoff, evaporation, film absorption and the distribution of the moisture in the wall (wetting-drying) (Fig. 2b and Fig. 3). These processes are also governed by all parameters that influence the impinging WDR intensity but also by additional parameters such as material properties and material surface characteristics including roughness, surface tension and surface soiling. At the scale of an individual raindrop, also the diameter, impact velocity and impact angle of each individual drop constituting the WDR are important parameters [110-112]. The wide range of influencing parameters indicates the complexity of the physical processes involved in rainwater runoff on building facades.

By far most research efforts on WDR in the past have focused on the first part of WDR assessment using three categories of methods: (1) measurements; (2) semi-empirical methods; and (3) numerical simulation based on Computational Fluid Dynamics (CFD). An extensive literature review on these methods and related previous research efforts was provided by Blocken and Carmeliet [5]. Later, in 2010, also a detailed comparison study of different semi-empirical and numerical (CFD) assessment methods was published [104], with applications for generic building configurations [105] and a real complex building for which a comparison with full-scale measurements was made [107].

Much less attention has been given to the second part of WDR research. This is not surprising, because research on the first part of WDR research is still in full development, while being an essential input to the second part of WDR research. This was already clearly stated by Couper in 1972 [113] in his paper on “Drainage from vertical surfaces”, and to a large extent, this statement is still valid today:

"More knowledge is needed about the distribution of driving rain, and especially the intensity of driving rain both in free air conditions and in its onslaught upon buildings…. A considerable amount of research work will be required before these data are available."

Nowadays, state-of-the-art hygrothermal analyses of building envelope systems are conducted with 1D, 2D or – exceptionally – also 3D HAM-models, and most of these models include WDR as a boundary condition. Examples are WUFI and WUFI ORNL/IBP [114,115], CHAMPS-BES (formerly called DELPHIN) [116,117], HYGirc [118-120] and HAMFEM [121]. To develop these models, several research efforts investigated the absorption and redistribution of WDR in porous building materials by measurements and/or simulations with HAM models (e.g. [110,111,114-138]). In some cases these HAM models have been equipped with WDR boundary conditions based on detailed CFD simulations of WDR on building facades [121,136-138]. However, to the best of our knowledge, currently none of the existing HAM models takes into account rainwater runoff. Nevertheless, several important research efforts on contact and surface phenomena have been made. Spreading, splashing and bouncing on building surfaces have been investigated by Couper [139], Abuku et al. [110,111] and Erkal et al. [112]. Abuku et al. [110,111] also analysed the differences between the so-called traditional approach of WDR in HAM simulations, in which the WDR intensity is applied as a uniform flux to a certain surface area, and the discrete approach, in which individual drops are allowed to impinge on the facade. Additionally, drop impact on impervious and porous solid surfaces was studied extensively in other research areas [140-169].

1.3. Scope and contents of the review

Given the complexity of WDR and the wide range of urban, building, material and meteorological parameters involved, it is not surprising that despite research efforts spanning over almost a century, WDR is still an active research subject in building physics and a lot of work remains to be done. Recent research efforts show that this includes both the first part (e.g. [106,107,170,171]) and the second part of WDR research (e.g. [50,112,172,173]). The present paper intends to contribute to ongoing research on the second part of WDR assessment by providing a detailed review of research on rainwater runoff on building facades. The review mainly focuses on the process of runoff itself. It starts with the definitions of rainfall, wind-driven rain and runoff and with information on wind flow around buildings and WDR impingement patterns, which is an essential prerequisite to understand and interpret rainwater runoff studies. Next, the review addresses the different assessment methods used in runoff research: field observations, field and laboratory experiments and analytical and numerical modelling. The review does not attempt to include the very large body of very valuable research efforts on the topic of water droplets impacting on surfaces and on the topic of rainwater absorption by porous building materials. It also does not focus on the topic of rain penetration through joints in masonry walls and curtain walls. The review will also not specifically focus on research topics where runoff is applied/involved, such as indirect evaporative cooling, self-cleaning action of surface coatings and leaching of surface coatings. However, it is important to note that the review does provide basic information on the boundary conditions necessary for studies of all these topics.

2. Definitions

2.1. Rainfall intensity and wind-driven rain intensity

We adopt the term "rain-intensity vector" from the literature on hydrology and earth sciences. It is defined as the vector of which the magnitude is the rainfall intensity (in L/m²h or mm/h) and the direction is that from which the rain is coming. In general, "WDR intensity" refers to the oblique rain vector. From the viewpoint of the interaction between rain and vertical building facades however, the term "WDR intensity" takes on the narrower meaning of "component of the rain vector causing rain flux through a vertical plane". The latter definition was adopted by the CIB (International Council for Building Research) [174] and is used in this paper. The other component of the rain-intensity vector, that causes rain flux through a horizontal plane, is termed (horizontal) rainfall intensity. Figure 4 clarifies the definitions of the rain-intensity vector, WDR and horizontal rainfall intensity. In Figure 4a, a homogeneous wind-flow field is considered. This means no disturbance of the flow field and -the same vertical profile of mean horizontal wind speed at every position. Let us assume that the rain behaves as if all drops were of the median size d_{50}. As a result of the homogeneous wind field, the raindrop trajectories are parallel (assuming a steady-state wind field). Two raindrop trajectories form a stream tube, the entrance and the exit of which are shown in the details 1 and 2. At a certain height above ground, the rain-intensity vector is $\overrightarrow{R_1}$. At the ground, it is $\overrightarrow{R_2}$. Mass conservation is expressed as:

$$\overrightarrow{R_1} \cdot \overrightarrow{A_h} = \overrightarrow{R_2} \cdot \overrightarrow{A_g} \quad (1)$$

where "$\cdot$" denotes the scalar product of the rain-intensity vector and the surface vector, A_h is the area of a horizontal surface at a certain height above ground and A_g is the area of the rain-gauge orifice. As the areas A_h and A_g are equal (parallel trajectories), following Eq. (1), the vertical components of both rain-intensity vectors are also equal and the flux $R_h.A_h$ is measured by the rain gauge. R_h is called the *horizontal* rainfall intensity (because it is measured by a gauge with a horizontal orifice; the definitions of measured rain intensity in hydrology are generally related to the gauge, not to the direction of the rain-intensity-vector component that is measured).

In Figure 4b, a building disturbs the wind flow. The wind field is no longer homogeneous and the raindrop trajectories are no longer parallel to each other. Mass conservation in the stream tube yields:

$$\overrightarrow{R_1} \cdot \overrightarrow{A_h} = \overrightarrow{R_3} \cdot \overrightarrow{A_f} \quad (2)$$

where A_f is an area on the building facade. According to the definition given above, the WDR intensity R_{wdr} is the horizontal component of the vector $\overrightarrow{R_3}$ (which causes the flux through the vertical plane). It is calculated from:

$$R_h A_h = R_{wdr} A_f \quad (3)$$

The rain amount is indicated by the symbol S (sum of rainfall in L/m² or mm). Several definitions have been used to describe the WDR intensity and the WDR sum on building facades. In this paper, we use the catch ratio η, which is defined as:

$$\eta(t) = \frac{R_{wdr}(t)}{R_h(t)} \quad (4)$$

Combining Eqs. (3) and (4), the catch ratio can be calculated based on the geometry of the stream-tube – again assuming a steady-state wind-flow field:

$$\eta(t) = \frac{A_h}{A_f} \quad (5)$$

This is called the "stream-tube" method. It is important to note that $R_h(t)$ is an "unobstructed" horizontal rainfall intensity, i.e. occurring outside the wind-flow pattern that is disturbed by the building (i.e. the rainfall that would be measured by a rain gauge placed in open field, as shown in Fig. 4a). In practical applications, the catch ratio will be measured and calculated for discrete time steps $[t_j, t_j+\Delta t]$ and is then redefined as:

$$\eta(t_j) = \frac{\int_{t_j}^{t_j+\Delta t} R_{wdr}(t)\,dt}{\int_{t_j}^{t_j+\Delta t} R_h(t)\,dt} = \frac{S_{wdr}(t_j)}{S_h(t_j)} \quad (6)$$

where $S_{wdr}(t_j)$ and $S_h(t_j)$ are the WDR sum and the unobstructed horizontal rainfall sum during time step $[t_j, t_j+\Delta t]$

The catch ratio is a complex function of the following parameters [5]: (1) urban geometry; (2) building geometry; (3) facade geometry; (4) position on the building facade, (5) wind speed, (6) wind direction, (7) horizontal rainfall intensity and (8) (horizontal) raindrop-size distribution. The parameters wind speed (m/s) and wind direction (degrees from north) are usually given as their values at 10 m height in the undisturbed flow (U_{10}, φ_{10}) and are then called reference wind speed and reference wind direction. U_{10} is the mean streamwise horizontal wind speed and φ_{10} is the direction from which the wind is coming. The parameter horizontal raindrop-size distribution $f_h(d)$ (m^{-1}) refers to the raindrop-size distribution falling through a horizontal plane (in the undisturbed flow field) [5].

2.2. Contact and surface phenomena including rainwater runoff

Part of the impinging WDR intensity on the building facade can be lost by splashing or bouncing (Fig. 2b and 3), while another part can evaporate, can spread on the surface, can be absorbed if the material is porous or remain stuck to the building facade by adhesion (e.g. [110,141]). Several droplets, especially if spreading occurs, can coalesce and eventually form a film. As the size of the coalesced droplets or the film thickness increases, gravity forces will eventually exceed surface tension forces, allowing the film to run down along the facade. Film runoff can be discontinuous, i.e. narrow streams of water running down, or continuous, i.e. the film has a width and length that are several orders of magnitude larger than the film thickness. Water running down or water pooling on quasi-horizontal surfaces can enter cracks or faulty junctions into the building envelope system, which is generally referred to as rain penetration. All these processes are accompanied by evaporation. In summary, the mass balance of a rain droplet is schematically represented in Figure 2b and expressed by Eq. (7):

$$V_{drop} = V_{splash} + V_{evap} + V_{abs} + V_{adh} + V_{runoff} \quad (7)$$

indicating that the volume of an impinging raindrop can undergo splashing, evaporation, absorption, adhesion and/or runoff.

3. Wind-driven rain impingement patterns and the wind-blocking effect

Knowledge of WDR impingement patterns on building facades is an essential prerequisite to study rainwater runoff. The literature review on the first part of WDR research [5] indicated that field measurements, wind-tunnel measurements and CFD simulations show a distinct WDR impingement pattern with large spatial gradients across the windward facade of a building. The top corners and the top edge of the windward facade receive the largest amounts of WDR. Later research work identified the wind-blocking effect as the main cause for the large WDR impingement gradients across the windward facade [100]. In this section, this effect is explained based on the results of previously performed CFD simulations of wind flow and WDR. These simulations were based on detailed grid-sensitivity analysis and were successfully validated with reduced-scale wind tunnel measurements [175] and field WDR measurements on two full-scale test buildings [97,98,100-103].

The CFD simulations were performed for four isolated buildings of different geometry (Fig. 5): (1) a low-rise cubic building (L x W x H = 10 x 10 x 10 m³); (2) a medium-rise wide slab (L x W x H = 100 x 10 x 20 m³); (3) a high-rise slab (L x W x H = 50 x 10 x 60 m³); and (4) a tower building (L x W x H = 20 x 20 x 80 m³). The simulations were performed for wind direction perpendicular to the wide/windward facade. First, the wind-flow pattern around the building was calculated by solving the 3D steady Reynolds-averaged Navier-Stokes (RANS) equations in combination with the realizable k-ε model by Shih et al. [176]. Next, raindrops with a wide range of diameters (0.3 mm – 6.0 mm) were injected in the calculated wind-flow pattern and their trajectories were obtained by solving the raindrop equations of motion (Lagrangian particle tracking). Finally, the catch ratios (η) were calculated from the raindrop trajectories using the "stream-tube method" (see section 2). Figure 6 shows particle trajectories of 1 mm raindrops in the U_{10} = 10 m/s flow field. Figure 7 displays the catch ratio contours across the windward facades, for U_{10} = 10 m/s and horizontal rainfall intensity R_h = 1 mm/h. Note that the catch ratio takes into account the whole spectrum of raindrop diameters [177]. More results can be found in [100]. For all buildings, the highest catch ratios are found at the top corners and top edge. However, the distribution of the catch ratio across the facade is quite different for each building. The reason is the so-called wind-blocking effect.

For isolated buildings and for WDR, the term "wind-blocking effect" refers to the upstream disturbance of the wind-flow pattern by the presence of the building and the associated decrease of the upstream streamwise wind-velocity component (wind-speed slow-down) [100]. As the streamwise wind speed decreases, so does the streamwise horizontal raindrop speed, which results in lower WDR intensities at the facade. The higher and the wider the building, the stronger this effect will be. Therefore, the wind-blocking effect also refers to decreased WDR exposure due to increased building dimensions (width and height). The low-rise cubic building A presents the least obstruction to the flow field, and therefore the raindrop trajectories are not much influenced by the local flow pattern around the building, as shown in Figure 6a. This results in high catch ratios at the top corners but also in high average catch ratio across the facade (Fig. 7a). The low-rise wide building B introduces a larger amount of wind-blocking, yielding more deflection of raindrop trajectories (Fig. 6b) and lower η-values, especially at the lower part of the facade (Fig. 7b). The high-rise wide building C presents the largest obstruction to the wind flow. The raindrop trajectories are to a large extent diverted away from the facade by the local wind-flow pattern (Fig. 6c). This large wind-blocking effect yields lower catch ratios at the top corners, but also very low catch ratio values at the lower part of the facade, which remains almost dry (Fig. 7c). Finally, the tower building D, although higher, is also much narrower, and the wind-blocking effect is present, although less pronounced as for building C (Figs. 6d, 7d). Note that the wind-blocking effect is not only found by CFD simulations but has also been confirmed by detailed WDR measurements on a building facade [100].

The wind-blocking effect is responsible for the counter-intuitive observation that the WDR exposure of a low-rise, cubic building (h = 10 m) can be larger than the WDR exposure of a high-rise building slab (h = 60 m) or even a high-rise tower building (h = 80 m). These observations appear to be in contrast to the general notion that the WDR exposure at the top of a building increases with the building height. This notion stems from the fact that the (free-field) wind speed increases with height and that higher wind-speed values yield higher WDR amounts. However, from an analysis of the simulated wind-flow patterns [100], it is clear that a wider and higher building represents a larger obstruction to the wind-flow pattern (wind blocking) which in turn can cause a lower WDR exposure, even at the top edge of the facade. On the other hand, it must be noted that the simulations were conducted for buildings without surrounding obstructions. In real built environments, buildings seldom stand alone. If we consider a typical European city with many low- and medium-rise buildings and with only a few high-rise buildings, the low-rise buildings will generally be sheltered from wind and rain by the surrounding buildings, while the few high-rise buildings will not be substantially sheltered. Therefore, the general notion that high-rise buildings are most exposed to WDR is in an urban context not necessarily wrong.

The wind-blocking effect has some important consequences for rainwater runoff. Runoff will start at the positions with the highest catch ratio. If the isolated buildings in Figure 5 are placed at the same location under the same meteorological conditions, rainwater runoff will occur first on the low-rise cubic building, next on the medium-rise wide slab and the tower building, and last on the high-rise slab. In addition, for the low-rise cubic model, the entire facade receives quite a large amount of WDR, which will promote rainwater runoff all along the wall down to the lowest part. For the high-rise slab, significant WDR impingement is only present near the top edge of the facade, and thus the rainwater film that would form at the top edge and run down would meet dry wall areas where mechanisms like adhesion and absorption can slow or stop the film progression, resulting in the absence of runoff usually observed at the foot of tall buildings. This knowledge on WDR impingement patterns and the wind-blocking effect will be used in the next sections to interpret results of rainwater runoff.

4. Field observations related to rainwater runoff

> *"Let us give back to our buildings the organs necessary for their defence against the weather: cornices, string-courses, architraves and mouldings, which allow a facade to remain what the artist intended it to be, in spite of the rain." (Perret in 1934, as cited by Collins in 1965 [178])*

In 1968, Sexton [179] published a pioneering study on "building aerodynamics" at the Building Research Station, following a presentation at the CIB Symposium on "Weathertight Joints for Walls" in Oslo in 1967. While most previous studies on building aerodynamics had focused on the assessment of wind loads (as part of "Structural Wind Engineering"), this particular study focused on air flow to support the analysis of rain penetration (as part of "Environmental Wind Engineering"). Figure 8 shows smoke injected into the airstream from small orifices in the windward face of a smooth-surfaced model in a wind tunnel. The figure shows that the flow spreads radially from the stagnation region. Based on this figure, Sexton [179] stated that it is likely that both rain drops in flight and water already deposited on the surface of a building will be carried by these surface airstreams, and that therefore surface details may have considerable effects on rain penetration of joints. Concerning raindrops in flight, this statement is in line with the CFD results in section 3 and has also been confirmed by many other studies of WDR [62-107]. Concerning the already deposited water (runoff water), this statement is supported by at least the measurements of rain penetration of joints in concrete panels by Bishop [180] and Bishop et al. [181], who showed that a large portion of water entering the joints flowed roughly horizontally across the panels. Rain penetration could therefore be reduced by providing projections at the vertical edges of the panels to prevent cross-flow of runoff water [179]. Other authors mentioning lateral flow of runoff water are Ritchie and Davison [182], Sasaki [183], Couper [113], Isaksen [184], Herbert [185], Robinson and Baker [186], Bielek [187], Baker [188] and El-Shimi et al. [189].

One of the first detailed written reports on observations of rainwater runoff and its consequences was provided by Couper [113] in 1972. Based on observations of buildings in Melbourne, Australia, he reported that runoff seldom occurs uniformly across the face of a building but rather in streams. The location of these streams appeared to vary from building to building, but most commonly occurred at the edges of the building and the surfaces of columns or other vertical discontinuities of the facade. He also stated that the uneven nature of the surface of any building naturally leads to the channelling of the rainwater runoff, and that this is assisted by the action of wind upon the building facade, which in turn may lead to transverse or even upward movement of the surface runoff. He stressed the importance of rainwater runoff by mentioning that, unfortunately, in most cases the runoff streams are located in areas where the risk of water penetration is high, such as vertical construction of expansion joints and the edges of window frames and sashes. His observations indicated that surface runoff at ground level did not occur on buildings of 10 or more storeys. Couper expected this to be caused by the fact that large volumes of water were either shed or absorbed and held by the buildings during rainstorms [113]. From the analysis in section 3 and from Figure 7, as explained above, it is clear that for such tall buildings, the wind-

blocking effect is pronounced and that it plays an important role in limiting runoff water from the facade.

In 1975, Robinson and Baker delivered an extensive report on the weathering of buildings based on a literature survey and on observations of buildings in Ottawa, Canada [186]. This report provides many important insights in rainwater runoff, and several of these are discussed below. Figure 9 (based on Fig. 12 from [186]) clearly shows the relationship between the WDR impingement patterns – as explained in section 3 – and the resulting rainwater runoff, also described in section 3. Robinson and Baker [186] also provided an interesting historical perspective related to changes in architectural design and their consequences for the weathering of the designed buildings due to rainwater runoff. They stated that, in the past, buildings were designed based on the knowledge of traditional, inherited practices in architecture, but that many modern architects, in their strive for plane, smooth building facades, chose to omit such details. In their enthusiasm in developing Modern Architecture, they have actually condemned old construction practice, without understanding that some of these traditions were actually beneficial from a building physics point of view. Evidence of this transition is not only based on observations of weathering of historical and contemporary building facades, but also on past publications. In 1908, Adolf Loos wrote an article called "*Ornament and Crime*", which was an assault on building facade details [190]. In addition, Le Corbusier in 1923 [191] defended the simplicity of forms (purism). Such points of view were rapidly taken on by developers after the Second World War. In too many cases, modern building design and construction have lead and – even today – continue to lead to buildings that in short periods of time show unacceptable surface soiling, weathering and decay. One example is the Royal Festival Hall shown in Figure 1. To counter this bleak picture, one should note that Modern ideas did not sweep all rational thinking. Auguste Perret, who was a much an architect as a constructor, provided the following reply to a questionnaire of 1934 entitled "*For or Against Ornament*" [178]:

> *"Let us give back to our buildings the organs necessary for their defence against the weather: cornices, string-courses, architraves and mouldings, which allow a facade to remain what the artist intended it to be, in spite of the rain".*

Clearly, part of the construction community realised that abandoning rain control by building facade design could be detrimental to the performance of their buildings. However, in the 70's, Robinson and Baker [186] stated that many modern designers were still not sufficiently aware of how natural forces act on their creations and could not predict with any certainty the results of their design decisions. They illustrated:

> "*… the ways in which the intentions of their designers had been negated, usually by the deposition of atmospheric dirt and its dispersal, often random, over wall surfaces by rain water." (Atkinson 1977 [192]).*

Unfortunately, this statement is almost equally valid today. In every city, buildings can be found that have suffered facade disfigurement by lack of control of rainwater runoff across the facade.

Robinson and Baker [186] correctly stressed that surface geometry such as horizontal and vertical projections or the sculpturing of the building panels, is the main means of controlling flow of runoff water, and that uncontrolled runoff will produce uneven weathering of building facades. While atmospheric deposition of dirt causes a fairly even degree of soiling, runoff can locally rinse away deposited dirt, causing light stains and streaks ("*white washing*") on the soiled surface. At other locations, this runoff water containing dirt particles can be absorbed, and this dirt will remain at least partly at the surface causing dirt stains and streaks ("*dirt washing*") (Fig. 10). The combination of white washing and dirt washing leads to the so-called "*differential surface soiling*", as shown in Figure 1 and Figure 10.

Related to the control of runoff water, Robinson and Baker [186] also provided information on the ability of runoff films to adhere to the underside of horizontal returns due to surface tension. Observations for a smooth granite facade showed that, at low rates of flow, a water film flows round the edge and along the underside of the horizontal return, and then on the adjacent vertical surface (Fig. 11). As the flow rate increases, the water begins to bead and drops from the underside of the return [186]. At higher flow rates, the momentum of the water film is sufficiently large to break the surface tension at the edge and to fall free [186]. In this perspective, the authors highlighted the importance of the drip and other design details with the same functionality, illustrating different design solutions to provide free dripping of runoff water (Fig. 12). One of the most common reasons for dirt marking on building facades is indeed "*the omission of drips from projecting horizontal elements or the provision of inadequate or incomplete drips*." [186]. This allows water to flow along the underside of horizontal surfaces and possibly on the adjacent vertical surfaces, resulting in an irregular flow pattern with associated irregular surface wetting and surface soiling (Fig. 1 and 10). A summary of the extensive report by Robinson and Baker [186] was provided by Baker [188].

It is important to note that the drip detail dates back to at least the Romans. In his "*Dictionnaire raisonné de l'architecture française du XIe au XVIe siècle*" (Dictionary of French Architecture from the 11th to the 16th

Century), the French architect Viollet-le-Duc (1814–1879) [193] provides a careful explanation of the drip detail accompanied by design drawings (Fig. 13). He defines the drip as "*a profile that forms a band or upper member of a cornice, and is intended to protect the facades by disposing the rain water away from the walls*". Figure 13 shows the drip of the Roman cornice, which leads the rainwater along the slope ab, around the edges bc and cd, and subsequently along the vertical face e, where it is then thrown off the wall. The absence of this detail allows the water to flow along the profiles without any obstruction and to reach the facade below. This effective detail drip has been used for centuries.

With the advent of new scientific knowledge, new materials and technology in the 19th and especially the 20th century, the fields of architecture and engineering began to separate, with some architects increasingly focusing on aesthetics at the expense of the technical aspects of building design. This is clearly illustrated by the abandonment of the drip detail by many architects in Modern Architecture at the turn of the 20th century, and by the above-mentioned article "*Ornament and Crime*" by Adolf Loos.

In 1980, El-Shimi et al. [189] published a detailed report of on-site observations of soiling patterns on buildings in downtown Montreal, Canada, addressing the relation between facade panel geometry and runoff and soiling patterns. A distinction was made between plain, moderately sculptured and heavily sculptured panels. For each panel type, the runoff behaviour was distilled from the observed soiling patterns. Also these authors provided several recommendations to limit surface soiling, several of which are directly linked to controlling runoff streams. Examples are avoiding horizontal sideways movement of rainwater and assuring continuous vertical flow by vertical dams and/or guided channels (Fig. 14), incorporating drips in soffits of horizontal projections, sideways and vertical draining of runoff from windows, etc.

In the last 20 years, rainwater runoff has continued to be studied. In their 1994 article on "Architectural detailing, weathering and stone decay", Mulvin and Lewis [194] stressed that 18th facade construction employed classical detailing for both decorative and utilitarian, protective functions, such as water flow control, where a considerable part of the rainwater was thrown off the building and one part of the building was sheltered by another. As a result, water penetration within the core fabric of the construction was minimized and the degradation of the materials upon which strength and structural integrity depends was lessened. Also more recent publications have confirmed the importance of facade detailing for controlling rainwater runoff and limiting facade surface soiling. Maurenbrecher [195,196] provides illustrations of frost damage, efflorescence and staining due to concentrated runoff on masonry walls due to faulty or absent detailing. He discusses how appropriate copings, sills with drips and flashings could have avoided these problems. Huberty and De Smet [43] addressed the surface soiling of concrete facades, Verhoef [44] reported on cleaning and soiling of building facades and Verhoef and Cuperus provided design guidelines for masonry facades [45]. Etyemezian et al. [46], Davidson et al. [47], Tang et al. [48] and Tang and Davidson [49] analysed surface soiling on the Cathedral of Learning, Pittsburg, based on measurements and CFD simulations of WDR impingement patterns. Chew and Tan [197] provided an overview of cases of rainwater runoff and the associated facade staining and also stressed the importance of controlling runoff flows to control staining and facade disfigurement.

A noteworthy fact is that many historical buildings not only display much less surface soiling due to the presence of water flow control features, but that surface soiling on their facades, when it does occur, is perceived as less disturbing by the human eye. This is attributed to the many protrusions and recessions of the facade details which cast a multitude of shadows across the facade that interact with and to some extent mask the soiled areas, see e.g. Figure 15a-c. Conversely, the abandonment of heavy detailing in modern architecture and the preference for plain and sometimes light-coloured surfaces and straight lines provides a perfect background to highlight differential surface soiling, as shown in Figure 15d-f.

On the related issue of wetting patterns, Küntz and van Mier [198] reported field observations of rainwater runoff on several small vertical concrete walls, focused on the development of the wetting front of water films running down from a top horizontal collecting surface. The horizontal surfaces were directly exposed to rainfall, as shown in Figure 16a, and horizontal rainfall was stated to largely predominate over WDR. As a result, the moisture flow along the concrete structures was essentially a 2D gravity-driven flow. The observations showed that the runoff wetting front may propagate in an unstable way by developing well defined and quite regularly spaced vertical finger-like features (Fig. 16b-c). These features are important because they allow a fast and large-distance runoff along these paths, resulting in heterogeneous distributions of moisture content across the wall and possibly large spatial deterioration gradients. Based on a brief theoretical analysis, Küntz and van Mier [198] stated that the development of an instable wetting front is driven by gravity but stabilized by capillary action. Figure 16b shows long and narrow "fingers" on a wall where capillary action is lower, while Figure 16c shows shorter and wider "fingers", suggesting that capillary action is more pronounced here. Note that the presence of these "fingers" is also clear from the photographs in Fig. 15d-f.

In summary, this section has shown that the rugged surface of traditional buildings, with their cornices and other apparently decorative features, has actually been shedding water and thus reducing the water load on the surface of thick loadbearing masonry walls which also provided, due to their absorption capacity, some buffering to rain penetration. The developments of Modern Architecture and the search for less expansive, thus lighter

construction systems coincided to generate a breed of sleek facades where junctions were often faced-sealed, a tactic that did not provide adequate water management. This section also has provided a non-exhaustive – but nevertheless representative of the literature – overview on the types of observations that have been made on rainwater runoff, often accompanied with a posteriori investigation of the reasons for differential surface soiling. These observations, mainly on damages and soiling, are important because they have provided and continue to provide very valuable qualitative, although indirect, information on runoff, which is very difficult or impossible to obtain in any other way, given the very wide range of influencing parameters.

5. Experiments of rainwater runoff

5.1. Field experiments

While the earliest WDR measurements on buildings can be traced back to Holmgren in 1937 in Trondheim, Norway [5], the first references – to the best of our knowledge – to runoff measurements on building walls are the reports by Ritchie and Davison [182] (National Research Council Canada, 1969), Harrison and Bonshor [199] (Building Research Station, UK, 1970) and Cronshaw [200] (Building Research Station, UK, 1971).

Ritchie and Davison [182] provided a brief and mainly qualitative report on measurements with WDR gauges and "run-off" gauges on two buildings, one in a continental climate (Ottawa, Ontario) and one in a maritime climate (Halifax, Nova Scotia). The walls of the Ottawa building were constructed of hollow clay tiles with an exterior finish of painted stucco, while the walls of the Halifax building were faced with sandstone slabs. The run-off gauges were thin rectangular metal boxes 305 mm (12 in.) long, 13 mm (½ in.) wide and 102 mm (4 in.) deep with an open top. They were attached and sealed to the wall with the long dimension horizontal. Water flowing down the wall surface entered the open top of the gauge, and was drained through a plastic tube into a collection bottle. The authors mentioned that the run-off measurements reflected the differences in wetting which occurred across the width of the facades and also indicated that a considerable portion of the rain was absorbed by the wall before it could flow down the surface and enter the gauge. Other quantitative information was not provided.

In 1970, Harrison and Bonshor [199] reported research focused on weatherproofing of joints, stressing the need for information about the "microclimates of joints" and the parameters for testing joints. Their report mentions a project by the Building Research Station (BRS) to measure runoff amounts on several buildings clad with different materials and equipped with "collecting gutters" and to relate these amounts to WDR measurements with traditional plate-type gauges. They also mentioned measurements at the Plymouth test rig of the BRS, to record the amount and spread of water penetrating into and through openings of various shapes and dimensions. The purpose of the Plymouth tests was to better understand and evaluate the principles of weather protection. While Harrison and Bonshor [199] did not present quantitative measurement results, they mentioned that the runoff amounts measured were considerably smaller than those used in runoff simulations in laboratory tests.

In 1972, Isaksen [184] very briefly mentioned the existence of field measurements on a column of 26 m high and 0.2 m width, but also this author provided no detailed information.

Cronshaw, in 1971 [200], provided some more information on the same BRS project as reported by Harrison and Bonshor [199]. He mentioned that the experiments were set up because of differences of opinion about runoff from wall surfaces. In particular, the project aimed at investigating the influence of surface textures and their effect on rainwater runoff. Measurements of WDR and runoff were made on four different walls. WDR was measured at 1 m below the top and 3 m above ground level, and runoff was measured only at 3 m above ground level. All positions were centrally in the width of the wall. The equipment to measure runoff was a rain collection gutter of 1 m length (Fig. 17). No other information and no quantitative results were reported, but the author emphasized that "*such simple studies can only be used to build up a very general picture of the situation, since there are many influences very difficult to identify accurately at the microscale*". From the experiments, Cronshaw [200] concluded that under conditions of moderate exposure, the run-off down the face of the wall is considerably less than the volume of WDR striking the wall, even when the latter is saturated.

To the knowledge of the authors, the most extensive field measurements of rainwater runoff were reported in 1976 by Beijer and Johansson [39] in a Swedish report that was briefly summarised in the English paper by Beijer [40] in 1977. Their intention was to provide information to explain surface soiling of facades due to rainwater runoff. For four buildings at four different locations in the Stockholm area, on-site measurements were made of impinging WDR intensities and of the resulting runoff amounts. Figure 18 shows one of the runoff gauges used. Some results for the building at the Södermalm site are discussed here. The building is located on a street in a central urban area, therefore the wall is somewhat sheltered from WDR. It is 20 m high and the facade exterior consists of concrete panels (Fig. 19a). No detailed information on the building geometry or on the surrounding buildings was provided. For the concrete panels, Beijer and Johansson [39] mentioned a value of the capillary absorption coefficient in dry conditions of 0.020-0.040 $kgm^{-2}s^{-0.5}$. However, they reported that, due to

initial moisture content, the actual values should be changed to about 0.007-0.020 kg/m²s$^{0.5}$ [39]. The positions of the WDR gauges and the runoff gauges are shown in Figure 19a and c. WDR was measured at five heights and runoff at four heights. Figure 19b shows the measured profiles of WDR intensity at the four sites. While Beijer and Johansson [39] reported several difficulties and problems associated with the measurements, there was one particular rain spell that was quite exceptional and also well recorded. This was the spell on 29th of September, 1973 : "*the driving rain exemplified had – and this was unusual – a fairly constant and considerable intensity for over an hour*" [39]. The corresponding WDR profile for the Södermalm site is indicated in Figure 19b. The measured WDR intensity, R_{wdr}, was 1 mm/h at a height of 18.5 m. Figure 19b clearly shows that the top of the facade receives most WDR, which is consistent with the information in Section 3 and with the "white washing" at the top of the facade as shown in Figure 19a and c. Figure 19d shows the measured (cumulative) runoff sum Q at different heights at 18, 36 and 72 min. after the start of the rain. As the top of the facade receives most WDR, runoff will start first at this position. As runoff accumulates on its way down, a maximum runoff rate is found at a certain distance from the top (Figure 19d), after which it decreases to zero, at the point where the surface is not yet capillary saturated and no runoff film has yet developed. Measured runoff was between 1-10 L/(mh), which indicates the volume of water passing a horizontal line of 1 m length, per hour. Note that Figure 19d also shows some calculation results, which will be addressed in Section 6 of this paper.

A different type of field experiments consists in simulated WDR and runoff on actual (on-site) building facades [12-14]. In addition, also laboratory experiments have been performed, which are briefly described in the next section.

5.2. Laboratory experiments

Laboratory experiments of rainwater runoff have been almost exclusively focused on testing rain penetration of different types of horizontal and vertical joints.

Sasaki [183] (1971) discussed the importance of laboratory tests for evaluating enclosure elements in terms of rain penetration. He addressed two water-leakage test methods used in North America: the static test and the dynamic test. An important requirement for a good rain penetration test is that it should simulate the lateral deflection of runoff water across the facade – as mentioned in section 4 – and its accumulation in vertical joints. While the static test cannot simulate these features, the dynamic test can reproduce pressure variations and lateral runoff flows. Wind is generated by a large fan that blows a high-velocity stream of air against the specimen surface. WDR can be simulated by injecting water drops into this air stream. Large water quantities will cause runoff. Runoff water can also be released at the top of the specimen. The lateral air streams cause lateral deflection of runoff water. Ishikawa [201] (1974) performed tests with a set-up similar to that of Sasaki [183].

Isaksen [184] (1972) reported the characteristics and the different development stages of the artificial wind and WDR chamber at the Norwegian Building Research Institute (NBRI) in Trondheim. The set-up included a side wind device, which applied gusts of horizontal wind parallel to the specimen surface, to study its effects on the lateral movement of runoff water. This NBRI set-up with side wind parallel to the facade was also used by Bielek [187] in 1977, who tested the lateral deflection of runoff water at a facade specimen with two protruding vertical nibs of different geometry. The results were converted into a chart, from which the optimal nib height can be extracted, as a function of wind speed, geometrical shape and surface texture.

A different type of laboratory test was reported by Couper [139] in 1974, who investigated the shedding of runoff water from various projection shapes. The amount of water shed was found to be a function of the shape and size of the projection and the velocity of the runoff water striking it.

Many other valuable laboratory experiments for rain penetration have been reported, only a few of which are mentioned here: Day et al. (1955 [202]), Skeen (1971 [203]), Vos and Tammes (1976 [204]), Beaulieu et al. (2001 [205]), Lacasse et al. (2003 [206]), Lacasse (2003 [207]) and Derome et al. (2007 [208]).

Baskaran and Brown (1995 [209]) examined three research facilities for – among others – rain penetration testing. Sahal and Lacasse (2008 [210]) provided an overview of water penetration test standards.

Apart from field measurements, Beijer [40] also performed laboratory tests of runoff on vertical surfaces of concrete, similar to those in the field experiments. He suggested Eq. (8) for the mean velocity of the film (v) in m/s:

$$v = 13\sqrt{q_1} \tag{8}$$

where q_1 is the runoff rate in m³/(ms), and Eq. (9) for the film thickness in mm:

$$d = 0.04\sqrt{q_2} \tag{9}$$

where q_2 is the runoff rate in L/(mh). These equations show that the maximum measured runoff amount of 10

L/(mh) corresponds to a local averaged runoff velocity of 80 m/h (0.022 m/s) (averaged over the height of the water film), and a runoff film thickness of about 0.12 mm. Note that these values are very small.

Finally, a few relatively new full-scale testing facilities for rainwater penetration testing facilities are mentioned (in alphabetical order): the Dynamic Wall Testing Facility of NRC-IRC [211], the Hurricane Simulator and High-Flow Loading Actuator at the University of Florida [212-215], the Insurance Institute for Business & Home Safety (IBHS) Research Center [216] and the Wall of Wind at Florida International University [217]. Some of these facilities are used for – among others – hurricane WDR research. In addition, the Insurance Research Lab for Better Homes at the University of Western Ontario [218-220] allows detailed investigation of the spatial variation of wind pressure and the development of naturally cracked wall panels and interfaces, which are important for WDR penetration research.

6. Analytical and numerical modelling of rainwater runoff

Only a limited number of analytical and numerical models for runoff have been developed in building engineering and building physics. They are generally combined with a water absorption model, because on many building facades absorption and runoff are coupled processes.

6.1. Analytical models of rain absorption and runoff

Analytical models of rain absorption and runoff were reported by Beijer and Johansson in 1976 [39], Beijer [40], El-Shimi et al. in 1980 [42], Hall and Kalimeris in 1982 and 1984 [122, 221] and Hall and Hoff in 2002 [131]. In 1976, Beijer and Johansson [39] proposed a simple analytical model for absorption, which is identical, as explained below, to the sharp front model described in detail by Hall and Hoff [131]. Beijer and Johansson [39] and Beijer [40] mentioned that the model is based on Eq. (10):

$$G_{abs} = A\sqrt{t} \tag{10}$$

where G_{abs} is the amount of water taken up by capillary action per surface unit (kg/m²), A is the capillary absorption coefficient (kg/ms$^{0.5}$) and t the time. However, care should be taken concerning the application of Eq. (10). Beijer and Johansson [39], Hall and Kalimeris [122, 221] and Hall and Hoff [131] correctly mention that Eq. (10) is only valid for free water uptake (in one direction into a homogeneously porous material), i.e. “full water provision” or “infinite water reservoir”, where the absorption flux is determined by the absorptive capacity by the material. However, especially for dry or nearly dry walls, the WDR intensity will generally be lower than the momentary absorptive capacity. In that case, all the impinging rainwater will be absorbed and this will continue until the WDR intensity exceeds the absorptive capacity. Note that this absorptive capacity decreases over time due to rainwater uptake, but that this decrease is not described by Eq. (10). This is in contrast to the model by El-Shimi et al. [189] that incorrectly assumes Eq. (10) to be valid during rainwater uptake, even at low WDR intensities.

The simplified WDR absorption by Beijer and Johansson [39] and Hall and Hoff [131] is briefly described below. It is based on the sharp front model in combination with a two-stage absorption process for walls wetted by WDR. Note that pressure infiltration, where wind or gravity pushes the film into the porous medium, is not considered here. Note that the capillary diffusivity D_w of most porous materials varies so strongly with liquid content that the capillary absorption profiles are often very steep-fronted [131], which justifies representing the wetted front region by a rectangular profile. This is the so-called Sharp Front (SF) approximation, which is essentially the Green-Ampt model of soil physics [222-224]. The SF model allows relatively simple analytical descriptions of many wetting processes, such as those of walls subjected to a constant WDR intensity. The basic assumption is that the wetted region can be considered as having a uniform and constant water content (i.e. the capillary water content w_c). Note that the validity of this model depends on the material type and that more complex models exist [114-138].

The first stage in the two-stage absorption process consists of WDR absorption by the wall with a constant flux boundary condition. As long as the moisture content at the wetted surface is below the capillary moisture content w_c, the absorption flux g_{abs} is equal to the supplied flux g_{wdr}, on condition that the supply flux is sufficiently small, which is generally the case for WDR and a relatively dry wall:

$$g_{abs} = g_{wdr} \tag{11}$$

For a constant WDR rate g_{wdr}, the cumulative amount of absorbed water at time t is:

$$G_{abs}(t) = g_{wdr}\, t \tag{12}$$

When w_c is reached, a water film is formed and the capillary uptake is similar to that from a liquid water surface. The time to film formation t_f depends on the WDR intensity and on the hydraulic properties of the material [131]:

$$t_f = \frac{A^2}{2 g_{wdr}^2} \tag{13}$$

Where A is the capillary absorption coefficient (kg/m²s$^{0.5}$). Starting from this moment, the boundary condition switches to a capillary saturation boundary condition. The WDR flux is then divided into two components: a part that is absorbed and a part which is in excess, and that runs off. At time t_f, the cumulative amount of absorbed water is:

$$G_{abs}(t_f) = g_{wdr}\, t_f = \frac{A^2}{2 g_{wdr}} \tag{14}$$

Hall and Hoff [131] indicate that, since SF water content profiles are always rectangular, the state of the system at t_f is identical with that which would be obtained if the surface had been put in contact with a free water reservoir (as in a sorptivity test) at some earlier time τ. The cumulative amount of absorbed water at that time is then given by [131]:

$$G_{abs}(\tau) = A\sqrt{\tau} \tag{15}$$

Combining Eq. (14) and Eq. (15) yields:

$$\tau = \frac{A^2}{4 g_{wdr}^2} = \frac{t_f}{2} \tag{16}$$

The origin of the time scale in the SF model is therefore situated halfway between t = 0 and t_f. The absorption flux for $t > t_f$ is:

$$g_{abs} = \frac{A}{2\sqrt{\left(t - \frac{t_f}{2}\right)}} \tag{17}$$

Note that the time t in Eq. (17) is the time from the start of the WDR event. Eq. (17) provides a continuous transition of the absorbed flux from Eq. (11) to Eq. (17). Some important limitations of this simplified model are mentioned:

1) The model assumes that, at the start of the rain event, the material is initially dry. If this is not the case, initial moisture content can be taken into account by lowering the capillary moisture coefficient A. This is the approach as used by Beijer and Johansson [39], Beijer [40] and Blocken and Carmeliet [50].
2) The model does not take limited material thickness into account. It assumes that, before and after surface saturation, the moisture front can freely penetrate into the material. Note however that this thickness is often very limited. Blocken and Carmeliet [50] found a maximum moisture front penetration depth of only 1.6 mm when simulating the experiments by Beijer and Johansson [39] for concrete panels (Figure 19).
3) The model assumes that capillary absorption itself is a 1D process, perpendicular to the wall surface, while in reality, some 2D effects will be present, although these have been shown to be limited for plane homogeneous walls [225].

For taking into account runoff, the 1D SF model needs to be extended with a 2D mass balance. This implies taking into account the rainwater runoff flux coming from higher facade parts in every calculation node or control volume on the facade. This can simply be done by adding the runoff flux q_{runoff} to the impinging WDR intensity g_{wdr}. The mass balances then allow calculating the film thickness h at every point along the wall.

Beijer and Johansson [39] compared this model to their rainwater runoff measurements (Fig. 19c). For the high initial moisture content prior to the measurements in Figure 19, laboratory measurements indicated A to be

0.007 kg/($m^2 s^{0.5}$). Using this model in combination with the WDR measurements in Figure 19b and the adjusted value for A, they obtained a good agreement between calculations and measurements for this particular rain spell with the quite steady WDR impingement rate (Fig. 19d).

Beijer [40] also used this model and the measured WDR intensity profiles (Fig. 19c) to develop a diagram that allows a rough estimate of the conditions for occurrence of rainwater runoff and the occurrence of rainwater runoff reaching the ground (bottom of the wall) (Fig. 20).

6.2. Numerical models for rain absorption

Already in 1982, Hall and Kalimeris [122] applied a dedicated finite element model to the unsaturated flow equation to determine absorption rates and runoff rates. The runoff was calculated based on the mass balance:

$$\frac{dh}{dx} = \frac{R_{wdr} - g_{abs}}{u} \tag{18}$$

where h is the film thickness (m), x the distance along the wall surface (downwards; m) and u the mean film velocity parallel to the surface. Based on this model, they found that runoff films are normally 0.1-0.3 mm thick with a mean runoff velocity of 0.025 to 0.25 m/s (90 to 900 m/h). Note that this corresponds to WDR intensities between 4 and 80 mm/h. These values agree well with those by Beijer [40] mentioned in section 5.2: local averaged runoff velocity of 0.022 m/s (80 m/h) (averaged over the height of the water film) and a runoff film thickness of about 0.12 mm. Hall and Kalimeris [221] also compared the absorption rates and runoff rates calculated by the finite element model with those obtained by the SF model, showing a close agreement.

Note that many other finite element or control volume models for rainwater absorption in porous materials were developed in the past decades [114-138]. These models reflect the current state of the art in modelling the combined heat, air and moisture transfer in porous building materials and building components and were listed above. However, at the time of writing this paper and to the best of our knowledge, none of these models include runoff models. In some of the models however, runoff is calculated to be removed from the rain load at the location of WDR impingement, although the runoff amount is not used as a supply term for lower facade parts.

6.3. Numerical model for runoff

In 2012, Blocken and Carmeliet [50] published their implementation of a simplified numerical model for rainwater runoff from building facades in combination with the simplified SF absorption model. The runoff model is represented by a first-order hyperbolic partial differential equation with the film thickness as primary variable. It was derived from the continuity equation, to which the WDR intensity and the capillary absorption flux by the wall are added as source and sink terms, and from the adoption of the parabolic velocity profile of the Nusselt solution as the film flow velocity profile (Fig. 21):

$$u(y) = \frac{g_r}{2\nu} \sin\beta \left(2h_N y - y^2\right) \tag{19}$$

In this equation, y is the coordinate perpendicular to the wall, g_r the gravitational constant (m/s²), ν the kinematic viscosity (m²/s), β the angle to the horizontal) and h_N the film thickness according to the Nusselt solution. The derivation of the Nusselt solution from the Navier-Stokes equations can be found in the literature (e.g. [226]). Strictly, the Nusselt solution is only valid for the thin film flow of an isothermal Newtonian liquid with constant density ρ and kinematic viscosity ν down an inclined plane under the action of gravity, where the flow is steady and parallel (laminar) and the film thickness is constant in space (no undulatory behaviour). It is assumed that the liquid surface is uncontaminated and that the air friction on the liquid surface is negligible. In addition, the spanwise gradients are assumed to be negligible, reducing the problem to 2D. The Nusselt solution therefore represents the flow of a film, with in-plane dimensions that are much larger than the film thickness. Eq. (19) was used to develop a transient equation describing the film thickness h as a function of the distance down the wall x and time t (Fig. 22, Eq. 20):

$$\frac{\partial h}{\partial t} + \frac{g_r h^2}{\nu} \frac{\partial h}{\partial x} = \frac{g_{wdr} - g_{abs}}{\rho} \tag{20}$$

Eq. (20) is a non linear, first order, hyperbolic partial differential equation with the film thickness h(x,t) as primary variable. Two major assumptions underlie this model: (1) the adoption of the Nusselt solution for

statistically-steady, developed films, in spite of actual wave behaviour, and (2) the adoption of the Nusselt solution for transient, developing films, in spite of the actual moving contact line complexity. Indeed, as opposed to the Nusselt conditions, the film thickness will generally not be constant and the flow will generally not be steady. It is expected that the Nusselt solution is most violated for developing films and for films with strong undulatory (wavy) behaviour. Both above-mentioned simplifications are directly related to surface tension effects and discussed in detail in [50].

Concerning the first assumption, strictly, the Nusselt solution is only applicable at very low Reynolds numbers (e.g. Re < 5). At higher Reynolds numbers, experiments as well as simulations by many authors (e.g. [227-236]) have shown that the flow is hydrodynamically unstable. In spite of the presence of waves, many authors have theoretically and experimentally confirmed that the Nusselt solution quite accurately describes the time-averaged film characteristics, such as the mean thickness and the mean velocity of the film, even though instantaneously, large deviations can occur [228,233-237]. It was shown that the Nusselt solution is a good approximation for representing the time-averaged properties of thin film flow, up to film Reynolds numbers of 1000. The relationship $Re_N = q_N/\nu$ implies that the Nusselt solution can thus be used up to runoff rates of q_N = 4705 L/mh, which is a very high threshold unlikely to be exceeded except for very exceptional WDR events.

Concerning the second assumption, it is unlikely that the Nusselt solution is valid at the moving film front of developing films. Because detailed experimental laboratory data on developing films could not be found in the published literature, Blocken and Carmeliet [50] performed a comparison study in which the results of the entire runoff model (including Nusselt solution and simplified SF absorption model) were compared with the experiments by Beijer and Johansson [39]. While it is recognized that these experimental data are not so comprehensive that this effort could be called "model validation", it was – at present and with the limited amount of available experimental data – considered a valuable effort in terms of at least model evaluation. The results in Figure 23 show a satisfactory agreement, taking into account the significant uncertainties involved in modelling the complex real-life runoff process. In addition, it is mentioned that the model is an integral model, in which at any time, mass is conserved. The calculated film thicknesses with this model also agreed well with the values measured by Beijer [40]: for Q_{runoff} = 1 L/mh: h_N = 0.041 mm versus h_{Beijer} = 0.048 mm; for Q_{runoff} = 10 L/mh: h_N = 0.104 mm versus h_{Beijer} = 0.128 mm. The above-mentioned facts therefore suggest that also the general downward movement of the film is predicted with fairly good accuracy

The results of the numerical model were also used to provide some insights in the runoff and absorption processes. Figure 24a repeats the profile of WDR intensity from the experiments by Beijer and Johanson [39]. Figure 24b illustrates the variation of the film thickness with time. Film formation only starts after about 3 min (see Eq. 13 with A = 0.006 kg/m²s$^{0.5}$ and g_{wdr} = 1.15 L/m²h at height 20 m), after which the film thickness continues to grow and the film travels down the wall. Film thickness growth is most pronounced during the first 12 minutes. The maximum film thickness during the rain spell is 0.077 mm. It was also found that at about 25 minutes after the start of the rain spell, the mean velocity of the film front decreases, due to the combined effect of larger absorption rates (larger A values) and lower WDR intensity at lower parts of the wall. The film does not reach the bottom part of the wall, not even after 72 minutes of uninterrupted WDR. Figure 24c shows the (cumulative) runoff sum Q and Figure 24d shows the (cumulative) sum of absorbed water Q_{abs} at different time steps. As long as runoff does not occur, the boundary condition at the wall is a flux boundary condition: all WDR is taken up by absorption; $g_{abs} = g_{wdr}$. This explains the similarity between the profiles of g_{wdr} and G_{abs} for the first few minutes. When runoff occurs, the boundary condition switched from a constant flux to a constant moisture content condition. The available supply of water for potential absorption is provided by both the impinging WDR and the runoff water from the higher part of the wall. The excess water – which is not absorbed – is added to the runoff sum Q.

Finally, note that another simplified model, for raindrop adhesion and runoff on non-porous material surfaces on a drop-by-drop basis, was developed and applied by Blocken and Carmeliet [238], and later extended by Carmeliet et al. [239] to include droplet evaporation. This model was used to study rainwater adhesion and runoff from window glass surfaces, to provide boundary conditions for glass staining. It was also used to assess the accuracy of WDR measurements by plate-type gauges, and to assess the evaporation of the impinged WDR raindrop from the gauge collection area [238].

7. Discussion

The intention of this paper was to provide a detailed review mainly focused on the process of runoff itself. It did not attempt to include the large body of research work on the topic of water droplet impact on surfaces or on the topic of rainwater absorption by porous building materials. It also did not focus on the topic of rain penetration through joints in masonry walls and curtain walls. The review did also not address research topics where runoff is applied and/or involved, such as indirect evaporative cooling, self-cleaning action of surface coatings and leaching of surface coatings. However, it is important to note that the review did provide basic information on the boundary conditions necessary for studies of these topics. Below, some additional considerations are

provided, as well as some directions for future research.

The information provided in this review paper serves to answer a frequently asked question amongst researchers and facade designers about runoff: "*When WDR hits a (non-porous) curtain wall of a high-rise building, when it subsequently runs down the wall and accumulates on its way down, why are large streams of rainwater run-off not observed at the bottom part of the facade (at street level)?*" Several answers have been suggested in the past, ranging from ''evaporation'' to ''splashing of rainwater running down the wall off the wall by small facade details''. Based on the present review of the state of the art, we believe that the right answer to this question is the combination of the type of WDR wetting pattern and the surface tension by which WDR water adheres to the walls. Concerning the wetting pattern, earlier research has indicated that it is highly non-uniform and that the top corners and top edges of building facades receive the highest WDR intensities. Moreover, recent research [100] has shown that especially for high and wide buildings, the lower facade parts receive much less WDR due to the wind-blocking effect. When runoff occurs on a facade with uniform material characteristics across the facade, it will generally start at the positions of highest WDR intensity, i.e. the top corners and top edges. The rainwater film that forms at these positions will then run down and meet dry wall areas where mechanisms like adhesion (and absorption for porous material surfaces) and evaporation can slow or stop the film progression.

Without attempting to be complete and focusing on the larger-scale process of runoff itself, which has also been the topic of this paper, the following main tasks for the future can be defined:

- Establishing high-quality experimental data sets of WDR impingement and WDR runoff on building facades composed of different materials. These data can be used to gain further insight in the processes of WDR impingement and runoff and to validate numerical models of runoff and rainwater absorption. To be suitable for validation, not only an assessment of measurement accuracy (and measurement errors) but also completeness of the data and complete reporting of the experimental conditions are essential. Completeness of the data refers to the fact that not only WDR and runoff on the facade need to be measured, but also reference wind speed, wind direction, horizontal rainfall intensity, temperature and relative humidity. Complete reporting of the experimental conditions refers to urban and building geometry, facade geometry, facade material characteristics, etc.
- Integrating runoff models in state of the art HAM codes. A particular challenge in this respect is the wide range of time scales that need to be covered in such simulations. While HAM transfer simulations (without WDR) are typically conducted at time steps of an hour (corresponding to the resolution of standard meteorological data), WDR uptake needs to be modelled with much smaller time steps, down to a few seconds [121]. Earlier runoff simulations [50] were based on time steps down to 0.01 s, although it should be mentioned that these were based on explicit rather than implicit discretisation. Nevertheless, efficiently addressing the wide range of time scales is an important challenge for implementation of runoff in HAM models. As a first step, the relatively simple runoff model presented in section 6.3 can be inserted into HAM codes. More complex runoff models including the effects of surface tension have been developed and applied in other research areas such as chemical and process engineering, and these models could also be integrated into HAM models. This will allow modelling the instability of wetting fronts and the formation of fingers, as shown in Figure 15d-f and Figure 16. However, it should be noted that the disciplines and situations in which these models have been applied so far are often subjected to much less influencing parameters than is the case for rainwater runoff on building facades. The very large number of influencing parameters for rainwater runoff and the resulting complexity and uncertainly could be an indication that less complex runoff models should be preferred, and that maybe the simple runoff model based on the Nusselt solution could be sufficient to extend state of the art HAM models with rainwater runoff.
- Investigating the importance of atmospheric parameters such as temperature and relative humidity on the rainwater runoff process, because these parameters can have a very large influence on the resulting moisture content of the wall.

8. Summary and conclusions

Rainwater runoff from building facades is a complex process governed by a wide range of urban, building, material and meteorological parameters. Given this complexity and the wide range of influencing parameters, it is not surprising that despite research efforts spanning over almost a century, wind-driven rain (WDR) and rainwater runoff are still very active research subjects. Accurate knowledge of rainwater runoff is important for hygrothermal and durability analyses of building facades, assessment of indirect evaporative cooling by water films on facades to mitigate outdoor and indoor overheating, assessment of the self-cleaning action of facade surface coatings and leaching of particles from surface coatings that enter the water cycle as hazardous pollutants. Research on rainwater runoff is performed by field observations, field measurements, laboratory measurements and analytical and numerical modelling.

Most research on rainwater runoff was based on field observations, which most often consisted of a posteriori investigation of the reasons for differential surface soiling. These observations have shown that runoff generally starts at the top of the facade, where WDR intensities are highest. Although it has been reported that runoff tends to occur in streams, the images of surface soiling patterns on facades generally seem to indicate a quite uniform wetting front, in which instabilities are visible as fingers but these do not extend down from the top of the facade. Field observations are very important because they have provided and continue to provide very valuable qualitative information on runoff, which is very difficult to obtain in any other way.

Only very little quantitative experimental information is available. The few quantitative field experiments that have been reported provide valuable information, but much more experimental data is needed to gain more insight in runoff processes and for validation of numerical models. In particular, given the very wide range of influencing parameters, it is important that future experimental campaigns give special attention to completeness of the data and experimental reporting, in which all relevant urban, building, facade and meteorological parameters are measured, documented and reported. Laboratory experiments allow reducing the number of influencing parameters, and can therefore provide important data for the initial understanding of runoff processes and for the initial validation of numerical models. However, a full validation study of numerical models should be based on field experiments, in which the models can be tested under the full range of influencing parameters.

Analytical and numerical modelling of runoff has so far been restricted to relatively simple models based on the Nusselt solution. More complex runoff models exist and have been developed and applied in other research areas such as chemical and process engineering. However, the situations in which these models have been applied are often subjected to much less influencing parameters than is the case for rainwater runoff on building facades. The very large number of influencing parameters for rainwater runoff and the resulting complexity and uncertainly could be an indication that less complex runoff models should be preferred, and that simplified models based on the Nusselt solution could be sufficient to extend state of the art HAM models with rainwater runoff. To the knowledge of the authors, current HAM models do not yet contain runoff models. The development, validation and implementation of runoff models into HAM models is an important task for the future.

Acknowledgements

The authors express their appreciation to the many researchers that have contributed to the current state of the art in research on wind-driven rain and rainwater runoff on building facades, many of which are cited in this paper. The authors also thank (1) White RB and Her Majesty's Stationary Office, for the permission to reproduce Figure 1; (2) Elsevier, for the permission to reproduce Figs. 3, 5, 6, 7, 21, 22, 23 and 24; (3) Building Research Establishment (BRE Garston, Watford, WD25 9XX, United Kingdom (copyright +44 (0)1923 664000)), for the permission to reproduce Fig. 8; (4) Canadian Science Publishing, for the permission to reproduce Figs. 14 and 15f; (5) HERON, for the permission to reproduce Fig. 16; (6) IHS Building Research Establishment Press for the permission to reproduce Fig. 17; (7) Swedish Cement and Concrete Research Institute (CBI) for the permission to reproduce Figs. 19 and 20.

References

[1] Marsh P. 1977. Air and rain penetration of buildings. The Construction Press Ltd., Lancaster, England. 174 p.

[2] Hutcheon NB. 1963. Requirements for exterior walls. Canadian Building Digests, CBD-48.

[3] Eldridge HJ. 1976. Common defects in buildings. HMSO, 486 p.

[4] Franke L, Schumann I, van Hees R, van der Klugt L, Naldini S, Binda L et al. 1998. Damage atlas: classification and analyses of damage patterns found in brick masrony. European Commission Research report nr. 8, vol. 2, Fraunhofer IRB Verlag

[5] Blocken B, Carmeliet J. 2004. A review of wind-driven rain research in building science. J Wind Eng Ind Aerodyn 92(13): 1079-1130.

[6] Day AG, Lacy RE, Skeen JW. 1955. Rain penetration through walls. A summary of the investigations made at the UK Building Research Station from 1925 to 1955. Building Research Station Note. No. C.364 (unpublished)

[7] Garden GK. 1963. Rain penetration and its control. Canadian Building Digest, Division of Building Research, National Research Council, CBD40, pp. 401-404

[8] Freeman IL. 1975. Building failure patterns and their implications. The Architects' Journal, Vol. 161, No. 6, February 1975, pp. 303-308

[9] Reygaerts J, Gasper M, Dutordoir C. 1976. 1200 problèmes. Erreurs de conception. Défauts de construction. Dégâts. (in French). Brussels, CSTC-revue, nr 3, September 1976

[10] Reygaerts J, Gasper M, Dutordoir C, Leblanc V. 1978. Comment éviter les dégâts (in French). Brussels, CSTC-revue, nr 3, September 1978

[11] Lacy RE. 1977. Climate and building in Britain. Her Majesty's Stationery Office, London

[12] Whiteside D, Newman AJ, Kloss PB, Willis W. 1980. Full-scale testing of the resistance to water penetration of seven cavity fills. Build Environ, Vol. 15, pp. 109-118

[13] Newman AJ, Whiteside D, Kloss PB, Willis W. 1982a. Full-scale water penetration tests on twelve cavity fills - Part I. Nine retrofit fills. Build Environ, 17(3), 175-191

[14] Newman AJ, Whiteside D, Kloss PB. 1982b. Full-scale water penetration tests on twelve cavity fills - Part II. Three built-in fills. Build Environ 17(3), 193-207

[15] Rousseau J. 1983. Rain penetration and moisture damage in residential construction. Building Science Insight '83, Seminar on Humidity, Condensation and Ventilation in Houses, Canada

[16] Pountney MT, Maxwell R, Butler AJ. 1988. Rain penetration of cavity walls: report of a survey of properties in England and Wales. Building Research Establishment Information Paper 2/88

[17] Briggen PM, Blocken B, Schellen HL. Wind-driven rain on the facade of a monumental tower: numerical simulation, full-scale validation and sensitivity analysis. Build Environ 2009; 44(8), 1675–1690.

[18] Price CA. 1975. The decay and preservation of natural building stone. Chemistry in Britain 11(10): 350-353

[19] Stupart AW. 1989. A survey of literature relating to frost damage in bricks. Masonry International 3(2): 42-50

[20] Maurenbrecher AHP, Suter GT. 1993. Frost damage to clay brick in a loadbearing masonry building. Can J Civil Eng, 20, 247-253

[21] Camuffo D, Del Monte M, Sabbioni C, Vittori O. 1982. Wetting, deterioration and visual features of stone surfaces in an urban area. Atmos Environ 16(9): 2253-2259.

[22] Charola AE, Lazzarini L. 1986. Deterioration of brick masonry caused by acid rain. ACS Symp. Series 318: 250-258

[23] Reddy MM, Youngdahl A. 1987. Acid rain and weathering damage to carbonate building stone. Mater Perform 26: 33-36

[24] Lipfert FW. 1989. Atmospheric damage to calcareous stones: comparison and reconciliation of recent experimental findings. Atmos Environ 23:415-429.

[25] Camuffo D. 1992. Acid rain and deterioration of monuments: how old is the phenomenon? Atmos Environ 26B: 241–247.

[26] Webb AH, Bawden RJ, Busby AK, Hopkins JN. 1992. Studies on the effects of air pollution on limestone degradation in Great Britain. Atmos Environ 26B: 165-181.

[27] Roels S, Carmeliet J, Hens H. 2003. Modelling unsaturated moisture transport in heterogeneous limestone - Part 1. A mesoscopic approach. Transp Porous Media 52(3): 333-350.

[28] Roels S, Carmeliet J, Hens H. 2003. Modelling unsaturated moisture transport in heterogeneous limestone - Part 2. Macroscopic simulations. Transp Porous Media 52(3): 351-369.

[29] Camuffo D, Sturaro G. 2001. The climate of Rome and its action on monument decay. Climate Research 16 : 145-155.

[30] Bravo AH, Soto AR, Sosa ER, Sánchez AP, Alarcón JAL, Kahl J, Ruíz BJ. 2006. Effect of acid rain on

building material of the El Tajín archaeological zone in Veracruz, Mexico, Environ Pollut 144: 655-660.
[31] Barrett D. 1998. The renewal of trust in residential construction, Commission of inquiry into the quality of condominium construction in British Columbia, Government of the Province of British Columbia.
[32] Morrison Hershfield Limited. 1996. Survey of Building Envelope Failures in the Coastal Climate of British Columbia, Canada Mortgage and Housing Corporation. B.C. and Yukon Regional Office, Morrison Hershfield Limited. The Office, Vancouver, British Columbia, 51 p.
[33] Karagiozis A, Desjarlais A. 2003. What influences the hygrothermal performance of stucco walls in Seattle. 9th Conference on Building Science and Technology, Vancouver, British Columbia, February 27-28, pp. 32-44.
[34] Teasdale-St-Hilaire A, Derome D. 2005. State-of-the-art review of simulated rain infiltration and environmental loading for large-scale building envelope testing. ASHRAE Transactions, vol. 111, part 2, Denver, Colorado, pp 389-401.
[35] Matthews RS, Bury MRC, Redfearn D. 1996. Investigation of dynamic water penetration tests for curtain walling. J Wind Eng Ind Aerodyn 60: 1-16.
[36] New Builder. 1991. 17 January.
[37] White RB. 1967. The changing appearance of buildings. HMSO, London, 64 p
[38] Robinson G, Baker MC. 1975. Wind-driven rain and buildings. Technical paper No. 445, Division of Building Research, National Research Council, Ottawa, Canada
[39] Beijer O, Johansson A. 1976. Driving rain against external walls of concrete. Swedish Cement and Concrete Research Institute. Research 7:76. Stockholm 1976, 92p
[40] Beijer O. 1977. Concrete walls and weathering. RILEM/ASTM/CIB Symp. on Evaluation of the Performance of External Vertical Surfaces of Buildings. Otaniemi, Espoo, Finland. August 28-31 and September 1-2, 1977, Vol. 1, pp. 67-76
[41] Baker MC. 1977. Rain deposit, water migration and dirt marking of buildings. RILEM/ASTM/CIB Symp. on Evaluation of the Performance of External Vertical Surfaces of Buildings. Otaniemi, Espoo, Finland. August 28-31 and September 1-2, 1977, Vol. 1, pp. 57-66
[42] El-Shimi M, White R, Fazio P. 1980. Influence of facade geometry on weathering. Can J Civil Eng, Vol. 7, No. 4, pp. 597-613.
[43] Huberty JM, De Smet R. 1980. Duurzaamheid van het uitzicht van dagvlakbeton. Het verouderen van gevels (in Dutch). Brochure WTCB-FeBe-VCN
[44] Verhoef LGW (editor). 1988. Soiling and cleaning of building facades. Report of the Technical Committee 62 Soiling and Cleaning of Building Facades (SCF) RILEM. Chapman and Hall, London
[45] Verhoef LGW, Cuperus YJ. 1993. Detailleren met baksteen. Voorkomen van visuele schade door vervuiling (in Dutch). Rapport 93-2 Civieltechnisch Centrum Uitvoering Research en Regelgeving – Koninklijk Verbond van Nederlandse Baksteenfabrikanten
[46] Etyemezian V, Davidson CI, Zufall M, Dai W, Finger S, Striegel M. 2000. Impingement of rain drops on a tall building. Atmos Environ 34: 2399-2412
[47] Davidson CI, Tang W, Finger S, Etyemezian V, Striegel MF, Sherwood SI. 2000. Soiling patterns on a tall limestone buildings: changes over 60 years. Environ Sci Technol 34(4): 560-565
[48] Tang W, Davidson CI, Finger S, Vance K. 2004. Erosion of limestone building surfaces caused by wind-driven rain. 1. Field measurements. Atmos Environ 38 (33): 5589-5599.
[49] Tang W, Davidson CI. 2004. Erosion of limestone building surfaces caused by wind-driven rain. 2. Numerical modelling. Atmos Environ 38 (33): 5601-5609.
[50] Blocken B, Carmeliet J. 2012. A simplified numerical model for rainwater runoff on building facades: possibilities and limitations. Build Environ 53: 59-73.
[51] CWCT 1994. Facade engineering - a research survey, Centre for Window and Cladding Technology, University of Bath, UK
[52] He J, Hoyano A. 2008. A numerical simulation method for analyzing the thermal improvement effect of super-hydrophilic photocatalyst-coated building surfaces with water film on the urban/built environment. Energy Build 40(6): 968-978.
[53] Saneinejad S, Moonen P, Defraeye T, Carmeliet J. 2011. Analysis of convective heat and mass transfer at the vertical walls of a street canyon. J Wind Eng Ind Aerodyn 99(4): 424-433.
[54] Saneinejad S, Moonen P, Defraeye T, Derome D, Carmeliet J. 2012. Coupled CFD, radiation and porous media transport model for evaluating evaporative cooling in an urban environment. J Wind Eng Ind Aerodyn 104–106: 455-463
[55] Chabas A, Lombardo T, Cachier H, Pertuisot MH, Oikonomou K, Falcone R et al. Behaviour of self-cleaning glass in urban atmosphere. Build Environ 43(12): 2124-2131.
[56] Euvananont C, Junin C, Inpor K, Limthongkul P, Thanachayanont C. TiO_2 optical coating layers for self-cleaning applications. Ceram Int 34(3): 1067-1071.

[57] Wangler TP. 2011. Modelling biocide release from architectural coatings. Chimica Oggi-Chemistry Today 29(6): 14-16.
[58] Wittmer IK, Scheidegger R, Stamm C, Gujer W, Bader HP. 2011. Modelling biocide leaching from facades. Water Research 45(11): 3453-3460.
[59] Burkhardt M, Zuleeg S, Vonbank R, Bester K, Carmeliet J, Boller M, Wangler T. 2012. Leaching of biocides from facades under natural weather conditions. Environ Sci Technol 46(10): 5497-5503.
[60] Coutu S, Rota C, Rossi L, Barry DA. 2012. Modelling city-scale facade leaching of biocide by rainfall. Water Res 46(11): 3525-3534.
[61] Vos BH. 1974. Introduction to the Second International Symposium on Moisture Problems in Buildings. 2nd International CIB/RILEM Symposium on Moisture Problems in Buildings. Rotterdam, The Netherlands, 10-12 September, 1974.
[62] Lacy RE. 1965. Driving-rain maps and the onslaught of rain on buildings. RILEM/CIB Symp. on Moisture Problems in Buildings, Rain Penetration, Helsinki, August 16-19, Vol. 3, paper 3-4
[63] Schwarz B. 1973. Witterungsbeanspruchung von Hochhausfassaden (in German). HLH (Heizung, Lüftung/Klimatechnik, Haustechnik), Bd. 24, Nr. 12, 376-384
[64] Schwarz B. 1973. Die Schlagregenbeanspruchung von Gebäuden. Messmethoden – Messgeräte (in German). In: Schlagregen. Messmethoden – Beanspruchung – Auswirkung. Institut für Bauphysik der Fraunhofer-Gesellschaft, Berlin 1973
[65] Sandberg PI. 1974. Driving rain distribution over an infinitely long high building: computerized calculations. 2nd International CIB/RILEM Symp. on Moisture Problems in Buildings. Rotterdam, The Netherlands, 10-12 September 1974, Paper 1-1-2
[66] Rodgers GG, Poots G, Page JK, Pickering WM. 1974. Theoretical predictions of rain drop impaction on a slab type building. Build Sci 9, 181-190
[67] Herbert MRM. 1974. Some observations on the behaviour of weather protective features on external walls. Building Research Establishment Current Paper, CP 81/74
[68] Jacobson L. 1977. Driving rain in vertical surfaces at CTH field station for building research and testing. RILEM/ASTM/CIB Symp. on Evaluation of the Performance of External Vertical Surfaces of Buildings. Otaniemi, Espoo, Finland. August 28-31 and September 1-2, 1977, Vol. 1, pp. 170-180
[69] Souster C. 1979. A theoretical approach to predicting snow loads and driving rain deposition on buildings. Ph.D. thesis, University of Sheffield, UK
[70] Ito H et al. 1983. Measurement of driving rain on external wall of a building (in Japanese). Proc. of the Annual Meeting of the Architectural Institute of Japan
[71] Hilaire J, Savina H. 1988. Pluie battante sur une facade d'immeuble (in French). EN-CLI 88.5 R, CSTB, Nantes
[72] Ishikawa H. 1988. Driving rain impaction on a high-rise building. Proc. Faculty of Engineering, Tokyo University, Japan, Vol. 14, 1-21
[73] Choi ECC. 1991. Numerical simulation of wind-driven-rain falling onto a 2-D building. Asia Pacific Conf. on Computational Mechanics, Hong Kong, pp. 1721-1728
[74] Choi ECC. 1993. Simulation of wind-driven-rain around a building. J Wind Eng Ind Aerodyn 46&47: 721-729
[75] Künzel HM. 1993. Rain loads on building elements. Contribution to the IEA-Annex-24 meeting, Report T2-D-93/02, Holzkirchen, October 1993
[76] Choi ECC. 1994. Determination of wind-driven-rain intensity on building faces. J Wind Eng Ind Aerodyn 51: 55-69
[77] Choi ECC. 1994. Parameters affecting the intensity of wind-driven rain on the front face of a building. J Wind Eng Ind Aerodyn 53: 1-17
[78] Surry D, Inculet DR, Skerlj PF, Lin J-X, Davenport AG. 1994. Wind, rain and the building envelope: a status report of ongoing research at the University of Western Ontario. J Wind Eng Ind Aerodyn 53: 19-36
[79] Inculet D, Surry D. 1994. Simulation of wind-driven rain and wetting patterns on buildings. BLWTL-SS30-1994. Final report
[80] Hens H, Ali Mohamed F. 1994. Preliminary results on driving rain estimation. Contribution to the IEA annex 24, Task 2 – Environmental conditions, T2-B-94/02
[81] Lakehal D, Mestayer PG, Edson JB, Anquetin S, Sini J-F. 1995. Eulero-Lagrangian simulation of raindrop trajectories and impacts within the urban canopy. Atmos Environ 29(23):3501-3517
[82] Sanders C. 1996. Heat, air and moisture transfer in insulated envelope parts: Environmental conditions. International Energy Agency, Annex 24. Final report, volume 2. Acco, Leuven, 1996.
[83] Sankaran R, Paterson DA. 1997. Computation of rain falling on a tall rectangular building. J Wind Eng Ind Aerodyn 72: 127-136

[84] Lammel G, Metzig G. 1997. Pollutant fluxes onto the facades of a historical monument. Atmos Environ 31 (15): 2249-2259
[85] Karagiozis A, Hadjisophocleous G, Cao S. 1997. Wind-driven rain distributions on two buildings. J Wind Eng Ind Aerodyn 67&68: 559-572
[86] Straube JF, Burnett EFP. 1997. Driving rain and masonry veneer. ASTM Symp. on Water Leakage Through Building Facades, Orlando, March 17 1996. Special Technical Publication, ASTM STP 1314, Philadelphia, 1997, pp. 73-87
[87] Kragh MK. 1998. Microclimatic conditions at the external surface of building envelopes. PhD thesis, Department of Buildings and Energy, Technical University of Denmark
[88] Straube JF. 1998. Moisture control and enclosure wall systems, PhD thesis, Civil Engineering, University of Waterloo, Ontario, Canada, 1998, 318 p.
[89] Högberg A. 1998. Microclimate description: To facilitate estimating durability and service life of building components exposed to natural outdoor climate. Chalmers University of Technology, Publication P-98:5.
[90] Högberg A. 1999. Microclimate measurement focused on wind-driven rain striking building surfaces. Proc. of the 5th Symp. on Building Physics in the Nordic Countries, Gothenburg, 24-26 August 1999, 369-376
[91] Hangan H. 1999. Wind-driven rain studies. A C-FD-E approach. J Wind Eng Ind Aerodyn 81: 323-331.
[92] van Mook FJR. 1999. Full-scale measurements and numeric simulations of driving rain on a building. 10ICWE, Copenhagen, Denmark, 21-24 June, 1145-1152
[93] van Mook FJR. 1999. Measurements and simulations of driving rain on the Main Building of the TUE. 5th Symp. on Building Physics in the Nordic Countries, Göteborg, Sweden, 24-26 August, 377-384
[94] Straube JF, Burnett EFP. 2000. Simplified prediction of driving rain on buildings. Proc. of the International Building Physics Conference, Eindhoven, The Netherlands, 18-21 September 2000, 375-382
[95] Inculet DR. 2001. The design of cladding against wind-driven rain. Ph.D. thesis, The University of Western Ontario, London, Canada, 297 p.
[96] van Mook FJR. 2002. Driving rain on building envelopes, PhD thesis, Building Physics and Systems, Eindhoven University of Technology, Eindhoven University Press, Eindhoven, The Netherlands, 2002, 198 p.
[97] Blocken B, Carmeliet J. 2002. Spatial and temporal distribution of driving rain on a low-rise building. Wind Struct5(5): 441-462.
[98] Blocken B, Carmeliet J. 2005. High-resolution wind-driven-rain measurements on a low-rise building – experimental data for model development and model validation. J Wind Eng Ind Aerodyn 93(12): 905-928.
[99] Blocken B, Carmeliet J. 2006. On the validity of the cosine projection in wind-driven-rain calculations on buildings. Build Environ 41(9): 1182-1189.
[100] Blocken B, Carmeliet J. 2006. The influence of the wind-blocking effect by a building on its wind-driven rain exposure. J Wind Eng Ind Aerodyn 94(2): 101-127.
[101] Blocken B, Carmeliet J. 2007. Validation of CFD simulations of wind-driven rain on a low-rise building. Build Environ 42(7): 2530-2548.
[102] Nore K, Blocken B, Jelle BP, Thue JV, Carmeliet J. 2007. A dataset of wind-driven rain measurements on a low-rise test building in Norway. Build Environ 42(5): 2150-2165.
[103] Abuku M, Blocken B, Nore K, Thue JV, Carmeliet J, Roels S. 2009. On the validity of numerical wind-driven rain simulation on a rectangular low-rise building under various oblique winds. Build Environ 44(3): 621-632.
[104] Blocken B, Carmeliet J. 2010. Overview of three state-of-the-art wind-driven rain assessment models and comparison based on model theory. Build Environ 45(3): 691-703.
[105] Blocken B, Deszö G, van Beeck J, Carmeliet J. 2010. Comparison of calculation methods for wind-driven rain deposition on building facades. Atmos Environ44(14): 1714-1725.
[106] Huang SH, Li QS. 2010. Numerical simulations of wind-driven rain on building envelopes based on Eulerian multiphase model. J Wind Eng Ind Aerodyn 98(12): 843-857.
[107] Blocken B, Abuku M, Nore K, Briggen PM, Schellen HL, Thue JV, Roels S, Carmeliet J. 2011. Intercomparison of wind-driven rain deposition models based on two case studies with full-scale measurements. J Wind Eng Ind Aerodyn 99(4): 448-459.
[108] Blocken B, Stathopoulos T, Carmeliet J, Hensen JLM. 2011. Application of CFD in building performance simulation for the outdoor environment: an overview. J Building Perform Simul 4(2): 157-184.
[109] Moonen P, Defraeye T, Dorer V, Blocken B, Carmeliet J. 2012. Urban physics: effect of the microclimate on comfort, health and energy demand. Frontiers of Architectural Research. In press. doi:10.1016/j.foar.2012.05.002

[110] Abuku M, Janssen H, Poesen J, Roels S. 2009. Impact, absorption and evaporation of raindrops on building facades, Build Environ 44(1): 113-124.
[111] Abuku M, Blocken B, Roels S. 2009. Moisture response of building facades to wind-driven rain: field measurements compared with numerical simulations. J Wind Eng Ind Aerodyn 97(5-6): 197-207.
[112] Erkal A, D'Ayala D, Sequeira L. 2012. Assessment of wind-driven rain impact, related surface erosion and surface strength reduction of historic building materials. Build Environ 57: 336-348
[113] Couper RR. 1972. Drainage from vertical faces. Symp. on Wind-driven rain and the multi-storey building, Division of Building Research, CSIRO, paper 4
[114] Künzel H, 1994. Simultaneous heat and moisture transport in building components. One- and two-dimensional calculation using simple parameters. PhD thesis, Universität Stuttgart, Germany.
[115] Künzel HM, Karagiozis A, Holm A, Desjarlais A. 2004. WUFI ORNL/IBP. Manual. Boundary and initial conditions. Fraunhofer Institut für Bauphysik.
[116] Grunewald J. 1997. Diffusiver und konvektiver stoff- und energietransport in kapillarporösen baustoffen. PhD thesis, Technische Universität Dresden, Dresden, Germany
[117] Grunewald J, Nicolai A. 2006. CHAMPS-BES. Version 1. Program for coupled heat, air, moisture and pollutant simulation in building envelope systems. User Manual. Building Energy and Environmental Systems Laboratory, Department of Mechanical and Aerospace Engineering, Syracuse University, NY.
[118] Cornick S, Maref W, Abdulghani K, van Reenen D. 2003. 1-D hygIRC: A simulation tool for modeling heat, air and moisture movement in exterior wallsIRC. Building Science Insight 2003 Seminar Series, National Research Council, Institute for Research in Construction, 10 pages (NRCC-46896 NB).
[119] Maref W, Cornick SM, Abdulghani K, van Reenen D. 2004. An advanced hygrothermal design tool "1-D hygIRC". eSim 2004 Conference, Vancouver, B.C, pp. 190-195 (NRCC-46902).
[120] NRC, 2007. hygIRC 1-D Version 1.0. User's Guide. National Research Council Canada. NRC-CNRC Construction.
[121] Janssen H, Blocken B, Carmeliet J. 2007. Conservative modelling of the moisture and heat transfer in building components under atmospheric excitation. Int J Heat Mass Transfer 50 (5- 6):1128-1140.
[122] Hall C, Kalimeris AN. 1982. Water movement in porous building materials–V. Absorption and shedding of rain by building surfaces. Build Environ 19: 13-20.
[123] Tammes E, Vos BH. 1984. Heat and Moisture Transfer in Building Constructions (in Dutch). Kluwer Technische boeken, 419 p.
[124] Sandin K. 1987. The moisture condition in aerated lightweight concrete walls. In situ measurements of the effect of the driving rain and the surface coating. Rapport TVBM – 3026. Division of Building Materials, Lund Institute of Technology, Sweden
[125] Künzel HM, 1993. Averaging climatic data and its effect on the results of heat and moisture transfer calculations. Fraunhofer-Institut für Bauphysik, Report T1-D-93/05, International Energy Agency – Annex 24 meeting, Holzkirchen, October.
[126] Sandin K. 1994. Moisture conditions in cavity walls with wooden framework. Building Research and Information 21, pp. 235-238
[127] Wilson MA, Hoff WD, Hall C, 1995. Water movement in porous building materials – XIII. Absorption into a two-layer composite. Build Environ 30: 209-219.
[128] Hens H. 1996. Heat, air and moisture transfer in insulated envelope parts: modelling. International Energy Agency, Annex 24. Final report, volume 1. Acco, Leuven. 1996.
[129] Künzel HM, Kiessl K. 1997. Calculation of heat and moisture transfer in exposed building components. Int J Heat Mass Transfer 40(1): 159-167.
[130] Brocken HJP. 1998. Moisture transport in brick masonry: the grey area between the bricks. Ph.D. thesis, Building Physics and Systems, Eindhoven University of Technology, The Netherlands.
[131] Hall C, Hoff WD. 2002. Water transport in brick, stone and concrete. Spon Press, London and New York.
[132] Dalgliesh WA, Surry D. 2003. BLWT, CFD and HAM modelling vs. the real world: Bridging the gaps with full-scale measurements. J Wind Eng Ind Aerodyn 91(12-15): 1651-1669.
[133] Karagiozis AN, Salonvaara M, Holm A, Kuenzel H. 2003. Influence of wind-driven rain data on hygrothermal performance, in: Proceedings of the Eighth International IBPSA Conference, Eindhoven, the Netherlands, 627-634.
[134] Hagentoft C-E, Kalagasidis AS, Adl-Zarrabi B, Roels S, Carmeliet J, Hens H. 2004. Assessment method of numerical prediction models for combined heat, air and moisture transfer in building components: benchmarks for one-dimensional cases. J Therm Envelope Build Sci 27(4): 327-352.
[135] Hens SLC. 2007. Building Physics – Heat, Air and Moisture. Wiley. Ernst and Sohn.
[136] Blocken B, Roels S, Carmeliet J. 2007. A combined CFD-HAM approach for wind-driven rain on building facades. J Wind Eng Ind Aerodyn 95(7): 585-607.

[137] Janssen H, Blocken B, Roels S, Carmeliet J. 2007. Wind-driven rain as a boundary condition for HAM simulations: analysis of simplified modelling approaches. Build Environ 42: 1555-1567.
[138] Abuku M, Janssen H, Roels S. 2009. Impact of wind-driven rain on historic brick wall buildings in a moderately cold and humid climate: Numerical analyses of mould growth risk, indoor climate and energy consumption. Energy Build 41(1): 101-110.
[139] Couper RR. 1974. Factors affecting the production of surface runoff from wind-driven rain. 2nd International CIB/RILEM Symp. on Moisture Problems in Buildings. Rotterdam, The Netherlands, September 10-12, 1974, paper 1.1.1
[140] Chandra S, Avedisian CT. 1992. Observations of droplet impingement on a ceramic surface. Int J Heat Mass Transf 35: 2377-2388.
[141] Rein M. 1993. Phenomena of liquid drop impact on solid and liquid surfaces. Fluid Dynamics Research 12: 61–93.
[142] Bennett T, Poulikakos D. 1993. Splat-quench solidification: estimating the maximum spreading of a droplet impacting a solid surface. J Mater Sci 28: 963–970.
[143] Mundo CHR, Sommerfeld M, Tropea C. 1995. Droplet-wall collisions: experimental studies of the deformation and breakup process. Int J Multiphas Flow 21: 151-173.
[144] Yarin AL, Weiss DA. 1995. Impact of drops on solid surfaces: self-similar capillary waves, and splashing as a new type of kinematic discontinuity. J Fluid Mech 283: 141-173.
[145] Healy WM, Hartley JG, Abdel-Khalik SI. 1996. Comparison between theoretical models and experimental data for the spreading of liquid droplets impacting a solid surface. Int J Heat Mass Transfer Mass Transfer 39(14): 3079–82.
[146] Range K, Feuillebois F. 1998. Influence of surface roughness on liquid water drop impact. J Colloid Interface Sci 203: 16-30.
[147] Rioboo R, Tropea C, Marengo M. 2001. Outcomes from a drop impact on solid surfaces. Atomization Sprays 11: 155-165.
[148] Roisman IV, Prunet-Foch B, Tropea C. 2002. Vignes-Adler M. Multiple drop impact on a dry solid substrate. J. Colloid Interface Sci. 256: 396-410.
[149] Alleborn N, Raszillier H, Anthonissen K, Lievens O. 2003. Spreading and sorption of a droplet on a porous substrate. In: Schweizer PM, Cohu O. (Eds). Proceedings of the 5th European Coating Symposium on Advances in Liquid Film Coating Technology, Fribourg, Switzerland, pp. 246–251.
[150] Reis NC, Griffiths RF, Santos JM. 2004. Numerical simulation of the impact of liquid droplets on porous surfaces. J Comput Phys 198: 747–70.
[151] Cossali GE, Marengo M, Santini M. 2005. Single-drop empirical models for spray impact on solid walls: A review. Atomization Sprays 15: 699-736.
[152] Weiss C. 2005. The liquid deposition fraction of sprays impinging vertical walls and flowing films. Int J Multiphas Flow 31: 115-140.
[153] Yarin AL. 2006. Drop impact dynamics: splashing, spreading receding, bouncing. Annual Review of Fluid Mechanics 38: 159–192.
[154] Zadrazil A, Stepanek F, Matar OK. 2006. Droplet spreading, imbibitions and solidification on porous media. J Fluid Mech 562: 1–33.
[155] Fujimoto H, Shiotani Y, Tong AY, Hama T, Takuda H. 2007. Threedimensional numerical analysis of the deformation behaviour of droplets impinging onto a solid substrate. Int J Multiphase Flow 33: 317–332.
[156] Attané P, Girard F, Morin V. 2007. An energy balance approach of the dynamics of drop impact on a solid surface. Phys Fluids. 19: 012101.
[157] Rioboo R, Voue M, Vaillant A, De Coninck J. 2008. Drop impact on porous superhydrophobic polymer surfaces. Langmuir 24(24): 14074-14077.
[158] Meng-Jiy W, Fang-Hsing L, Yi-Lin H, Lin SY. 2009. Dynamic behaviors of droplet impact and spreading: water on five different substrates. Langmuir 25(12): 6772-6780.
[159] Tsai P, Pacheco S, Pirat C, Lefferts L, Lohse D. 2009. Drop impact upon micro- and nanostructured superhydrophobic surfaces. Langmuir 25(20): 12293-12298.
[160] Kuo-Long P, Chun-Yu H. 2010. Droplet impact upon a wet surface with varied fluid and surface properties. J Colloid Interf Sci 352(1): 186-193.
[161] Gupta A, Kumar R. 2010. Droplet impingement and breakup on a dry surface. Comput Fluids 39(9): 1696-1703.
[162] Castrejon-Pita JR, Betton ES, Kubiak KJ, Wilson MTC, Hutchins IM. 2011. The dynamics of the impact and coalescence of droplets on a solid surface. Biomicrofluidics 5(1): 014112.
[163] Marengo M, Antonini C, Roisman IV, Tropea C. 2011. Drop collisions with simple and complex surfaces. Current Opinion in Colloid & Interface Science 16(4): 292-302.
[164] Ping-ping C, Xi-shi W. 2011. Experimental study of water drop impact on wood surfaces. Int J Heat Mass Transfer 54(17-18): 4143-4147.

[165] Smith MI, Bertola V. 2011. Particle velocimetry inside Newtonina and non-Newtonian droplets impacting a hydrophobic surface. Exp Fluids 50(5): 1385-1391.
[166] Ellis AS, Smith FT, White AH. 2011. Droplet impact on to a rough surface. Q J Mech Appl Math 64(2): 107-139.
[167] Sang Mo A, Sang Yong L. 2012. Maximum spreading of a shear-thinning liquid drop impacting on dry solid surfaces. Exp Therm Fluid Sci 38: 140-148.
[168] Sungjune J, Hutchings IM. 2012. The impact and spreading of a small liquid drop on a non-porous substrate over an extended time scale. Soft Matter 8(9): 2686-2696.
[169] Palacios J, Hernandez J, Pablo G, Zanzi C, Lopez J. 2012. On the impact of viscous drops on dry smooth surfaces. Exp Fluids 52(6): 1449-1463.
[170] Giarma C, Aravantinos D. 2012. Estimation of building components' exposure to moisture in Greece based on wind, rainfall and other climatic data. J Wind Eng Ind Aerodyn 99(2-3): 91-102.
[171] Pérez-Bella JM, Domínguez-Hernández J, Rodríguez-Soria B, del Coz-Díaz JJ, Cano-Suñén E. 2012. Estimation of the exposure of buildings to driving rain in Spain from daily wind and rain data. Build Environ 57: 259-270.
[172] Carmeliet J, Derome D. 2012. Temperature driven inward vapor diffusion under constant and cyclic loading in small-scale wall assemblies: Part 1 experimental investigation. Build Environ 48: 48-56.
[173] Carmeliet J, Derome D. 2012. Temperature driven inward vapor diffusion under constant and cyclic loading in small-scale wall assemblies: Part 2 heat-moisture transport simulations. Build Environ 47: 161-169.
[174] Birkeland O. 1965. General report. Rain penetration. RILEM/CIB Symp. on Moisture Problems in Buildings, Rain Penetration, Helsinki, August 16-19, Vol. 3, paper 3-0
[175] Blocken B, Dezsö G, van Beeck J, Carmeliet J. 2009. The mutual influence of two buildings on their wind-driven rain exposure and comments on the obstruction factor. J Wind Eng Ind Aerodyn 97(5-6): 180-196.
[176] Shih TH, Liou WW, Shabbir A, Yang Z, Zhu J. 1995. A new k-ε eddy viscosity model for high Reynolds number turbulent flows. Comput Fluids 24: 227-238.
[177] Best AC. 1950. The size distribution of raindrops. Q J R Meteorolog Soc 76: 16-36.
[178] Collins P. 1965. Changing Ideals in Modern Architecture. 1750-1950. Montreal, McGill University Press.
[179] Sexton, DE. 1968. Building Aerodynamics. Current Paper 64/68, Building Research Station, also In: Proceedings of the CIB Symposium on Weathertight Joints for Walls, Oslo, September 25–28, 1967.
[180] Bishop D. 1962. An interim report of joints between concrete panels. D.S.I.R., Building Research Station, Note No. C861, Jan. 1962.
[181] Bishop D, Webster CJD, Herbert MRM. 1968. The performance of drained joints. Paper No. 64c, CIB Report No. 11, Jan. 1968.
[182] Ritchie T, Davison JI. 1969. The wetting of walls by rain. Internal report No. 367, Division of Building Research, National Research Council, Ottawa, Canada
[183] Sasaki JR. 1971. Testing building enclosure elements for rain penetration. National Research Council of Canada, Division of Building Research, Technical Paper, Vol. 334, 8 p.
[184] Isaksen T. 1972. Driving rain and joints: testing of model joints between elements. Norwegian Building Research Institute, 30 p.
[185] Herbert MRM. 1974. Some observations on the behaviour of weather protective features on external walls. Building Research Establishment current paper, 81/74, 17 p.
[186] Robinson G, Baker MC. 1975. Wind-driven rain and buildings. National Research Council of Canada, Division of Building Research, Technical Paper No. 445, Ottawa, July 1975.
[187] Bielek M. 1977. The main principles of water movement on the wall surfaces of building of various roughnesses. RILEM/ASTM/CIB Symposium on Evaluation of the Performance of External Vertical Surfaces of Buildings. Otaniemi, Espoo, Finland. August 28-31 and September 1-2, 1977, Vol. 1, pp. 77-96.
[188] Baker MC. 1977. Rain deposit, water migration and dirt marking of buildings. RILEM/ASTM/CIB Symposium on Evaluation of the Performance of External Vertical Surfaces of Buildings. Otaniemi, Espoo, Finland. August 28-31 and September 1-2, 1977, Vol. 1, pp. 57-66.
[189] El-Shimi M, White R, Fazio P. 1980. Influence of facade geometry on weathering. Can J Civil Eng 7(4): 597–613.
[190] Collins P. 1959. Concrete: the Vision of a New Architecture. New York Horizon Press, 1959.
[191] Le Corbusier. Toward an Architecture (Verse une Architecture). Translated by John Goodman. Los Angeles: Getty Research Institute, 2007.
[192] Atkinson GA. 1977. External vertical surfaces of buildings: aspects of design and appearance. RILEM/ASTM/CIB Symposium on Evaluation of the Performance of External Vertical Surfaces of Buildings. OTANIEMI, Espoo, Finland. August 28-31, 1977, and September 1-2, 1977, Volume 1.

[193] Viollet-le-Duc E. Dictionnaire raisonné de l'architecture française du XIe au XVIe siècle, Tome 6, A. Morel editor, Paris, 1868.
[194] Mulvin L, Lewis JO. 1994. Architectural detailing, weathering and stone decay. Build Environ 29(1): 113-138.
[195] Maurenbrecher AHP. 1998. Water-shedding details improve masonry performance. Construction Technology Update, No. 23, Institute for Research in Construction, National Research Council Canada.
[196] Maurenbrecher AHP. 1999. Protecting masonry from water run-off. Solplan Review, September 1999, Institute for Research in Construction, National Research Council Canada, pp. 16-17
[197] Chew MYL, Tan PP. 2003. Facade staining arising from design features. Constr Build Mater 17:181-187.
[198] Küntz M, van Mier JGM. 1997. Field evidences and theoretical analysis of the gravity-driven wetting front instability of water runoffs on concrete structures. Heron, 42(4): 231-244.
[199] Harrison HW, Bonshor RB. 1970. Weatherproofing of joints: a systematic approach to design. Ministery of Public Building & Works, Building Research Station, UK, Current Papers, 29/70
[200] Cronshaw JL. 1971. Rainwater run-off from walls. London, Building. 12 February 1971, 7/123
[201] Ishikawa H. 1974. An experiment on mechanism of rain penetration through horizontal joints in walls, Proceedings of the 2nd International CIB/RILEM Symposium on Moisture Problems in Buildings, Rotterdam, 10-12 September 1974.
[202] Day AG, Lacy RE, Skeen JW. 1955. Rain penetration through walls. Garston, Building Research Station Note C.364 (unpublished).
[203] Skeen JW. 1971. Experiments on the rain penetration of brickwork: the effect of mortar type. Building Research Station Current Paper 33/71.
[204] Vos BH, Tammes E. 1976. Rain penetration through the outer walls of cavity structures. CIB W40 Washington Meeting.
[205] Beaulieu P, Cornick SM, Dalgliesh WA, Djebbar R, Kumaran MK et al. 2001. MEWS methodology for developing moisture management strategies: application to stucco-clad wood-frame walls in North America, September 01, NRCC-45213, 21 p.
[206] Lacasse MA, O'Connor T, Nunes SC, Beaulieu P. 2003. Report from Task 6 of MEWS Project : experimental assessment of water penetration and entry into wood-frame wall specimens. Final Report, Research Report No. 133, Institute for Research in Construction, National Research Council of Canada, 308 p.
[207] Lacasse MA. 2003. Recent studies on the control of rain penetration in exterior wood-frame walls. BSI 2003 Proceedings, Oct., 15 cities across Canada, pp. 1-6.
[208] Derome D, Desmarais G, Thivierge C. 2007. Large-scale experimental investigation of wood-frame walls exposed to simulated rain penetration in a cold climate. Proceedings of Thermal Performance of the Exterior Envelopes of Whole Buildings X Conference, DOE/ORNL/ASHRAE/BETEC/ABAA, December 2-7, Clearwater Beach, FL, U.S.A., ASHRAE, 9 p.
[209] Baskaran BA, Brown WC. 1995. Dynamic evaluation of the building envelope for wind and wind driven rain performance. J Therm Insul Build Envelopes 18: 261-275.
[210] Sahal N, Lacasse MA. 2008. Proposed method for calculating water penetration test parameters of wall assemblies as applied to Istanbul, Turkey. Build Environ 43(7):1250-1260.
[211] Lacasse MA. 2004. IRC studies on the control of rain penetration in exterior wood-frame walls. Solplan Review, no. 14, January 2004, pp. 14-15.
[212] Masters FJ, Gurley KR, Prevatt DO. 2008. Full-scale simulation of turbulent wind-driven rain effects on fenestration and wall systems, 3rd International Symposium on Wind Effects on Buildings and Urban Environment, March 4-5, 2008, Tokyo, Japan.
[213] Salzano CT, Masters FJ, Katsaros JD. 2010. Water penetration resistance of residential window installation options for hurricane-prone areas. Build Environ 45(6): 1373-1388.
[214] Lopez C, Masters FJ, Bolton S. 2011. Water penetration resistance of residential window and wall systems subjected to steady and unsteady wind loading. Build Environ 46(7):1329-1342.
[215] Balderrama JA, Masters FJ, Gurley KR, Prevatt DO, Aponte-Bermúdez LD, Reinhold TA et al. 2011. The Florida Coastal Monitoring Program (FCMP): A review. J Wind Eng Ind Aerodyn 99(9): 979-995.
[216] http://disastersafety.org/research-center/. Retrieved on October 10, 2012.
[217] Bitsuamlak GT, Chowdhury AG, Sambare D. 2009. Application of a full-scale testing facility for assessing wind driven rain intrusion. Build Environ 44(12): 2430-2441.
[218] Bartlett FM, Galsworthy JK, Henderson D, Hong HP, Iizumi E, Inculet DR et al. 2007. The Three Little Pigs Project: a new test facility for full-scale small buildings. 12th International Conference on Wind Engineering, (12ICWE), 2-6 July 2007, Cairns, Australia.
[219] Kopp GA, Morrison MJ, Henderson DJ. 2012. Full-scale testing of low-rise, residential buildings with realistic wind loads. J Wind Eng Ind Aerodyn 104–106: 25-39.

[220] Morrison MJ, Kopp GA. 2011. Performance of toe-nail connections under realistic wind loading. Engineering Structures 33(1): 69-76
[221] Hall C, Kalimeris AN. 1984. Rain absorption and runoff on porous building surfaces. Can J Civ Eng 11: 108-111.
[222] Green WH, Ampt GA. 1911. Studies on soil physics. Part 1. The flow of air and water through soils. J Agric Sci 4: 1-24.
[223] Philip JR. 1969. Theory of infiltration. Advances in Hydrosciences 5: 215-296.
[224] Marshall TJ, Holmes JW, Rose CW. 1996. Soil physics, 3rd Edition, Cambridge University Press.
[225] Janssen H, Carmeliet J. 2006. Hygrothermal simulation of masonry under atmospheric excitation. In: Fazio et al. (Eds.), Research in Building Physics and Building Engineering, Taylor & Francis, London, pp. 77-82.
[226] Ruyer-Quil C, Manneville P. 1998. Modeling film flows down inclined planes. Eur Phys J B 6: 277-292.
[227] Krantz WB, Goren SL. 1971. Stability of thin liquid films flowing down a plane. Indust Engng Chem Fundam 10, 91-101.
[228] Takahama H, Kato S. 1980. Longitudinal flow characteristics of vertically falling liquid films without concurrent gas flow. Int J Multiphase Flow 6: 203-215.
[229] Alekseenko SV, Nakoryakov VY, Pokusaev BG. 1985. Wave formation on a vertical falling liquid film. AIChE J. 31, 1446-1460.
[230] Liu J, Paul JD, Gollub JP. 1993. Measurements of the primary instabilities of film flows. J Fluid Mech 250: 69-101.
[231] Ramaswamy B, Chippada S, Joo SW. 1996. A full-scale numerical study of interfacial instabilities in thin-film flows. J Fluid Mech 325: 163-194.
[232] Kapitza PL. 1948. Wave flow of thin layers of a viscous liquid. Zh Eksperim I Teor Fiz, Vol. 18. Translated in: Collected Papers of P.L. Kapitza, edited by D. Ter Haar, Pergamon, New York, 1965, pp. 662–689.
[233] Kapitza PL, Kapitza SP. 1949. Wave flow of thin layers of a viscous liquid. Zh. Eksperim. I. Teor. Fiz., Vol. 19. Translated in: Collected Papers of P.L. Kapitza, edited by D. Ter Haar, Pergamon, New York, 1965, pp. 690–709.
[234] Mudawar I, Houpt RA. Measurement of mass and momentum transport in wavy-laminar falling liquid films. Int J Heat Mass Transfer 36(17): 4151-4162.
[235] Karimi G, Kawaji M. 1998. An experimental study of freely falling films in a vertical tube. Chem Eng Sci 53(20): 3501-3512.
[236] Moran K, Inumaru J, Kawaji M. 2002. Instantaneous hydrodynamics of a laminar liquid film. Int J Multiphase Flow 28: 731-755.
[237] Ambrosini W, Forgione N, Oriolo F. 2002. Statistical characteristics of a water film falling down a flat plate at different inclinations and temperatures. Int J Multiphase Flow 28: 1521-1540.
[238] Blocken B, Carmeliet J. 2006. On the accuracy of wind-driven rain measurements on buildings. Build Environ 41(12):1798-1810.
[239] Carmeliet J, Rychtarikova M, Blocken B. 2006. Numerical modeling of impact, runoff and drying of wind-driven rain on a window glass surface. 3rd International Building Physics Conference (3IBPC), August 27-31 2006, Montreal, Quebec, Canada, pp. 905-912.

FIGURE CAPTIONS

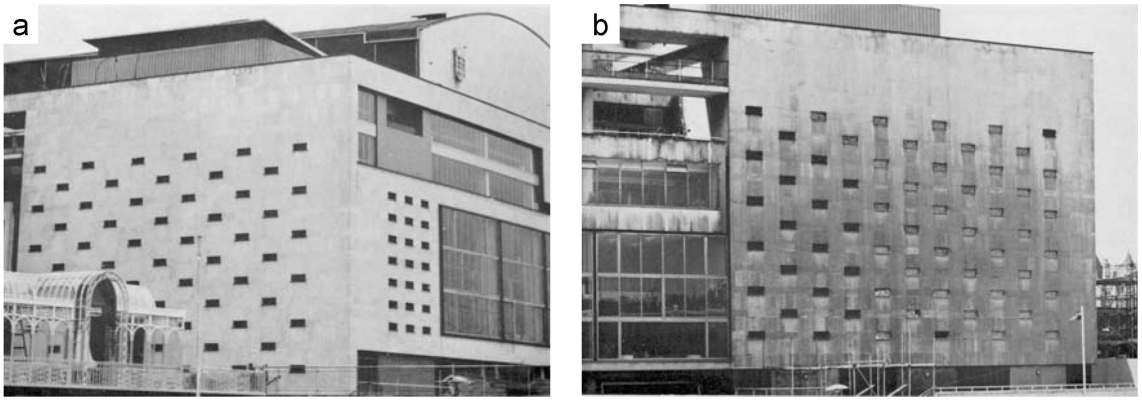

Figure 1: Royal Festival Hall, London. (a) After building completion. (b) After a few years of exposure to atmospheric pollution and wind-driven rain deposition and runoff across the facade (from [37], reproduced with permission).

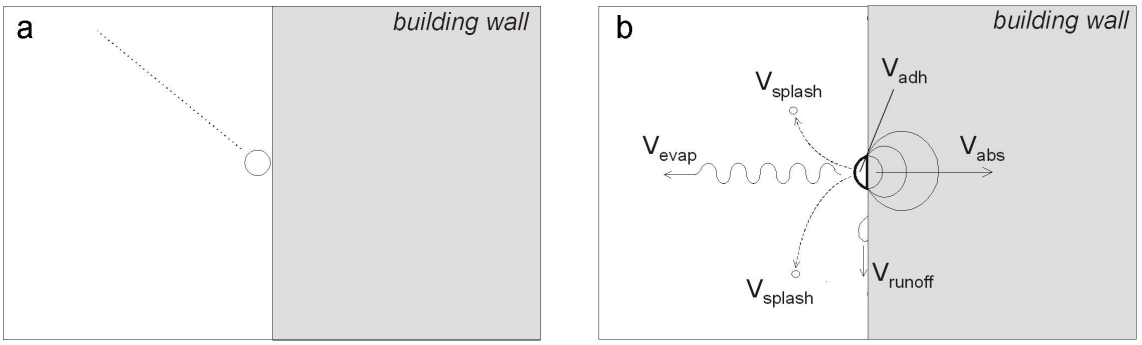

Figure 2: Schematic representation of the two parts in wind-driven rain research: (a) assessment of the impinging wind-driven rain intensity (before raindrop impact) and (b) assessment of the response of the building wall (at and after raindrop impact).

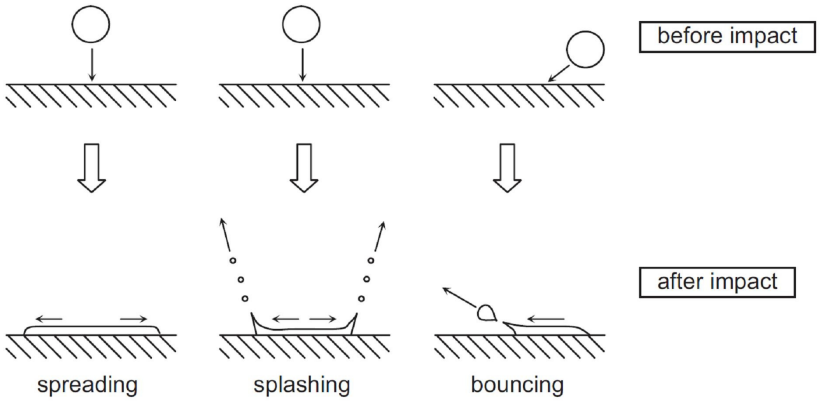

Figure 3: Schematic representation of spreading, splashing and bouncing of a raindrop on a solid and dry surface (from [110], reproduced with permission).

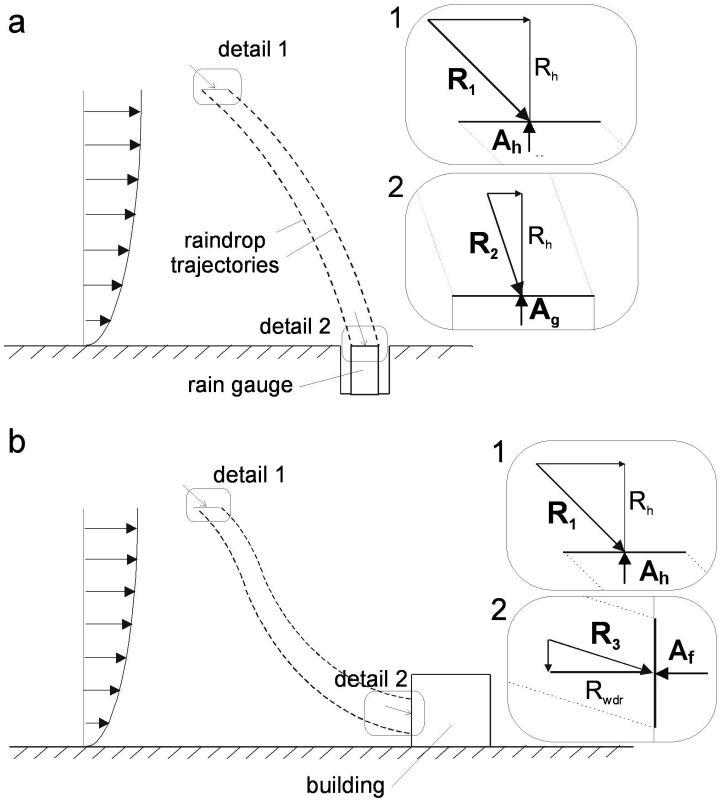

Figure 4: (a) Definition of horizontal rainfall intensity. The rain falls to the ground in homogeneous wind conditions and the raindrop trajectories are parallel to each other. (b) Definition of wind-driven rain intensity on a building. Raindrop trajectories are not parallel to each other.

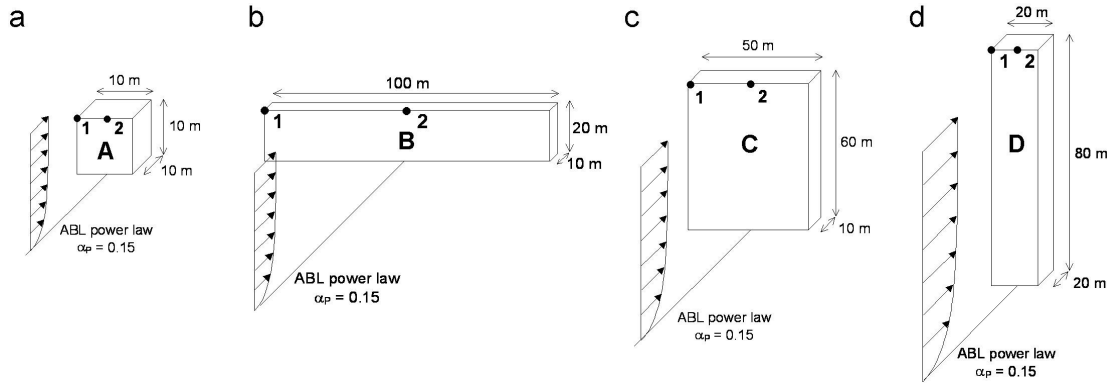

Figure 5. Building configurations and dimensions for study of the wind-blocking effect: (a) Low-rise cubic building: LxBxH = 10x10x10 m³; (b) Wide medium-rise building slab: LxBxH = 100x10x20 m³; (c) High-rise building slab: LxBxH = 50x10x60 m³; (d) Tower building: LxBxH = 20x20x80m³ (based on [100], reproduced with permission).

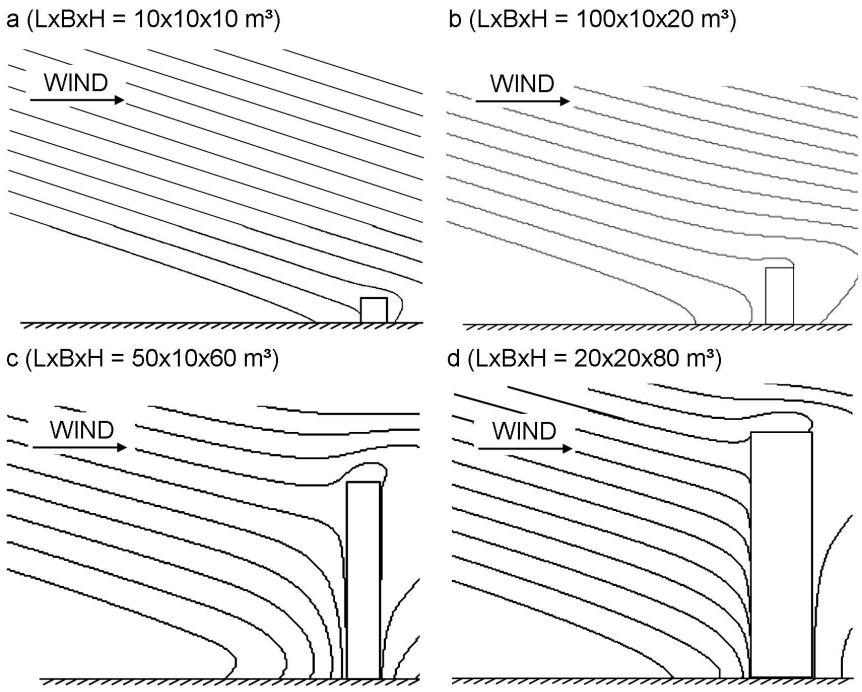

Figure 6. Trajectories of 1 mm diameter raindrops in the U_{10} = 10 m/s wind flow pattern in a vertical plane through the centre of the building (based on [100], reproduced with permission).

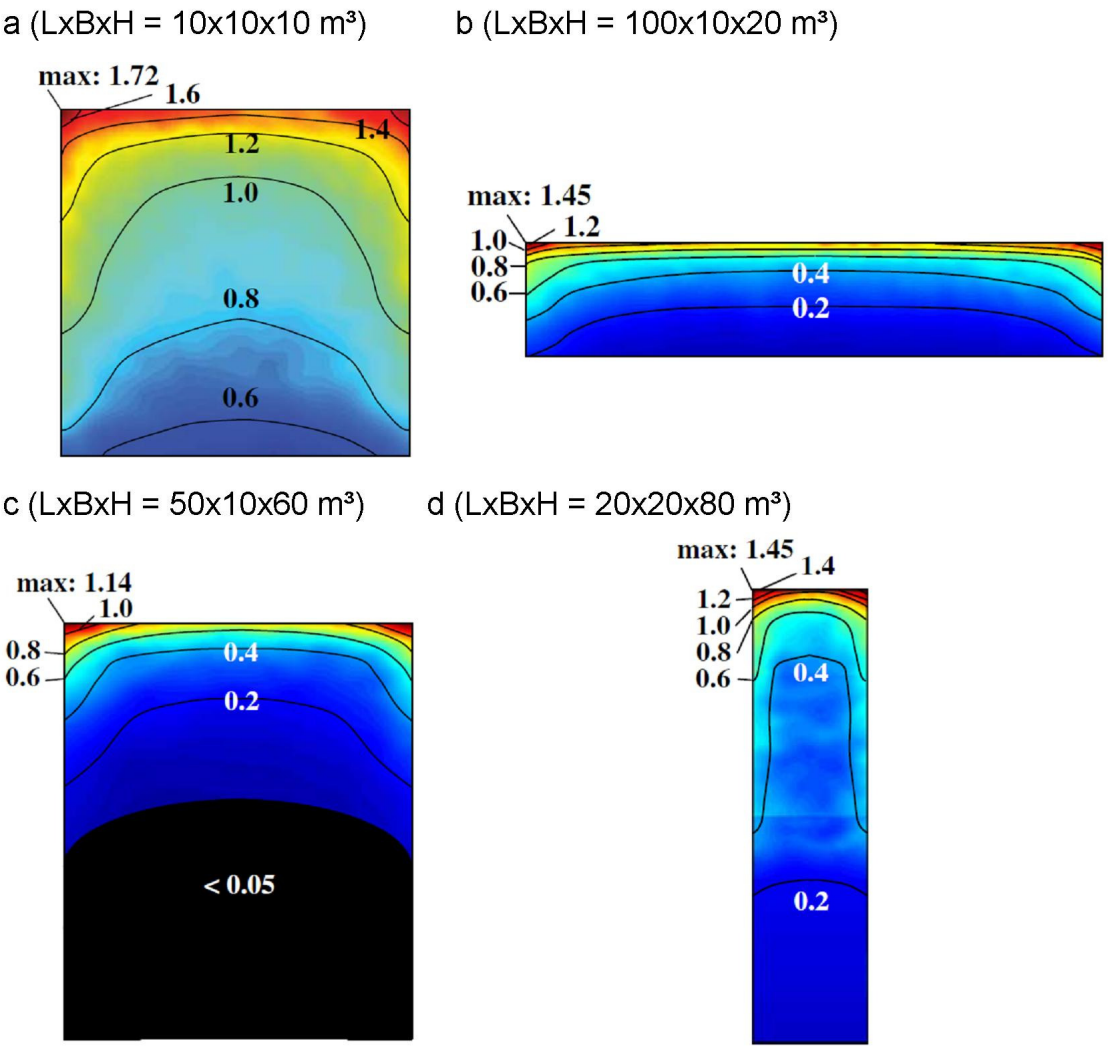

Figure 7. Spatial distribution of the catch ratio across the windward facade for the four building configurations, for reference wind speed U_{10} = 10 m/s and horizontal rainfall intensity R_h = 1 mm/h (based on [100], reproduced with permission).

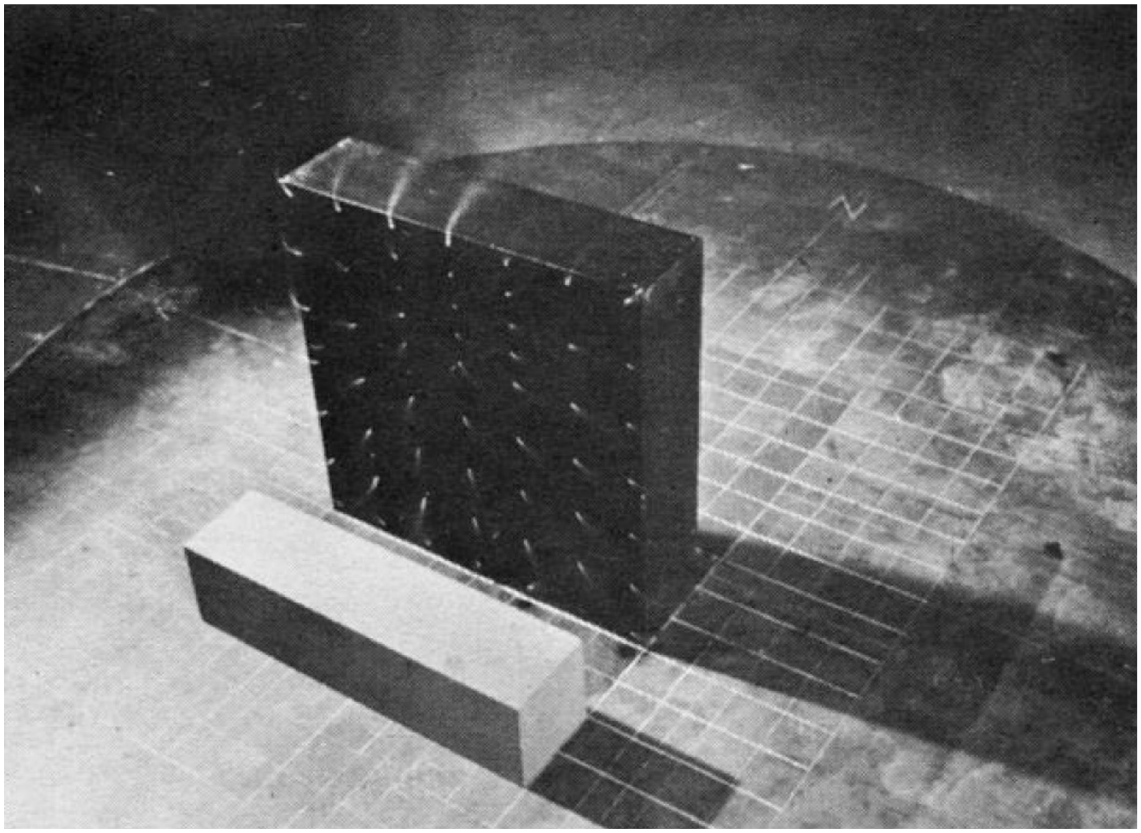

Figure 8. Smoke visualization test in a wind tunnel. Smoke is injected into the airstream from small orifices in the windward face of the slab illustrating the division of the flow (from [179], reproduced with permission)

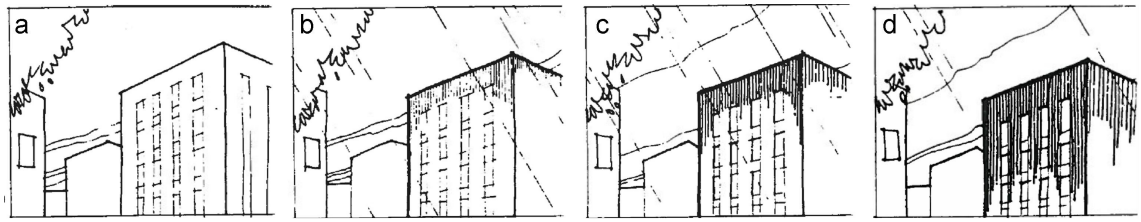

Figure 9. Artist impression of observed rainwater runoff on a windward building facade (from [186]).

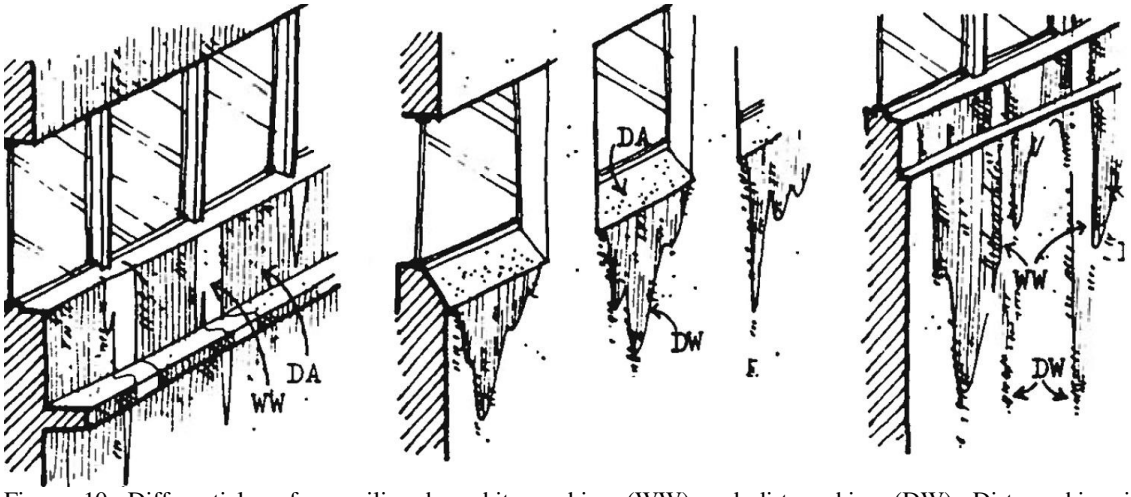

Figure 10. Differential surface soiling by white-washing (WW) and dirt-washing (DW). Dirt washing is preceded by runoff over surfaces with dirt accumulation (DA) (from [186]).

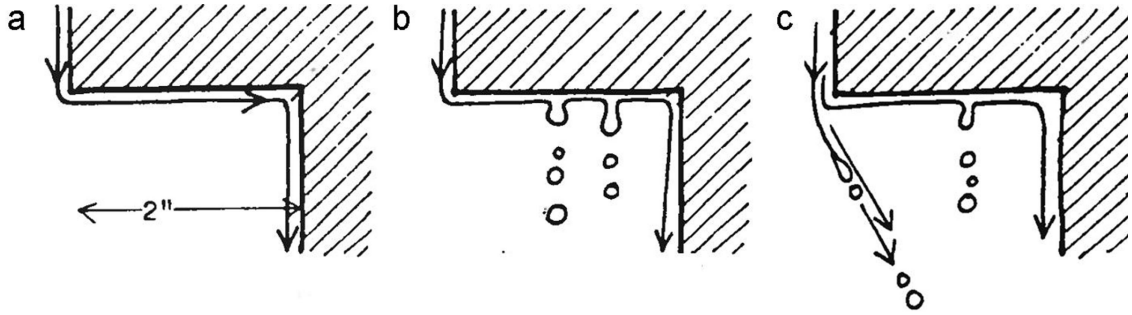

Figure 11. Vertical cross-sections with indication of surface tension effects for (a) low, (b) moderate and (c) high runoff flow rate (from [186]).

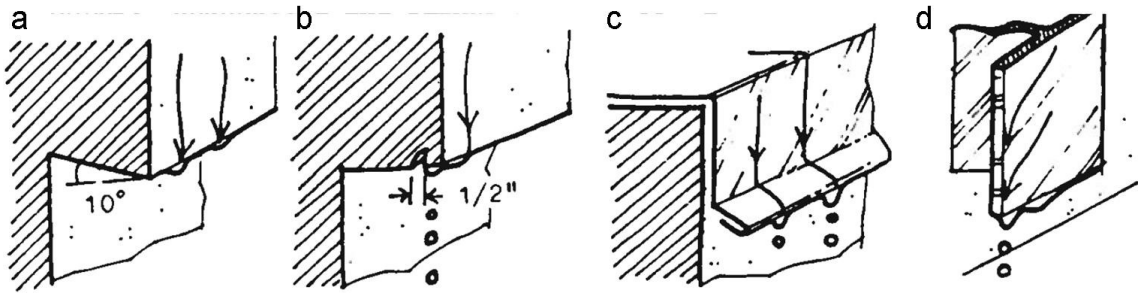

Figure 12. Design details for free dripping of runoff water at a discontinuity: (a) inclined soffit; (b) drip detail; (c) flashing; (d) T-mullion (from [186]).

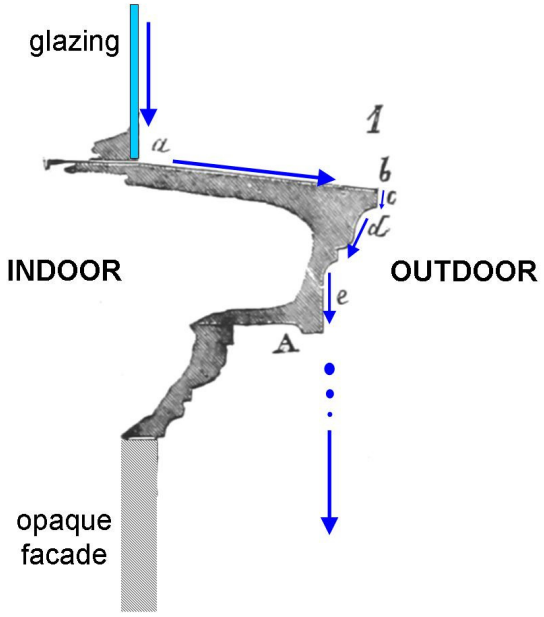

Figure 13. Modified design drawing of drip detail by Viollet-Le-Duc (Dictionnaire raisonné de l'architecture française du XIe au XVIe siècle, Tome 6) (modified from [193]).

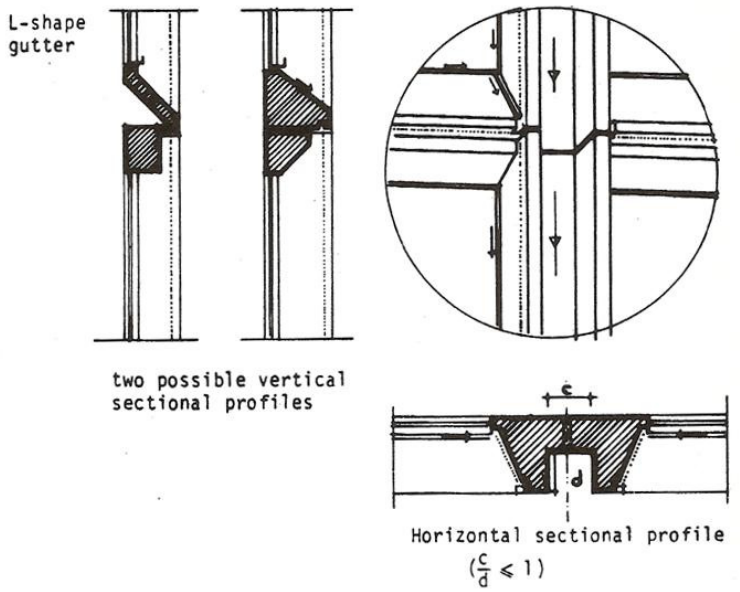

Figure 14. Example of a recommended profile type for vertical guidance of runoff streams by El-Shimi et al (from [189], reproduced with permission).

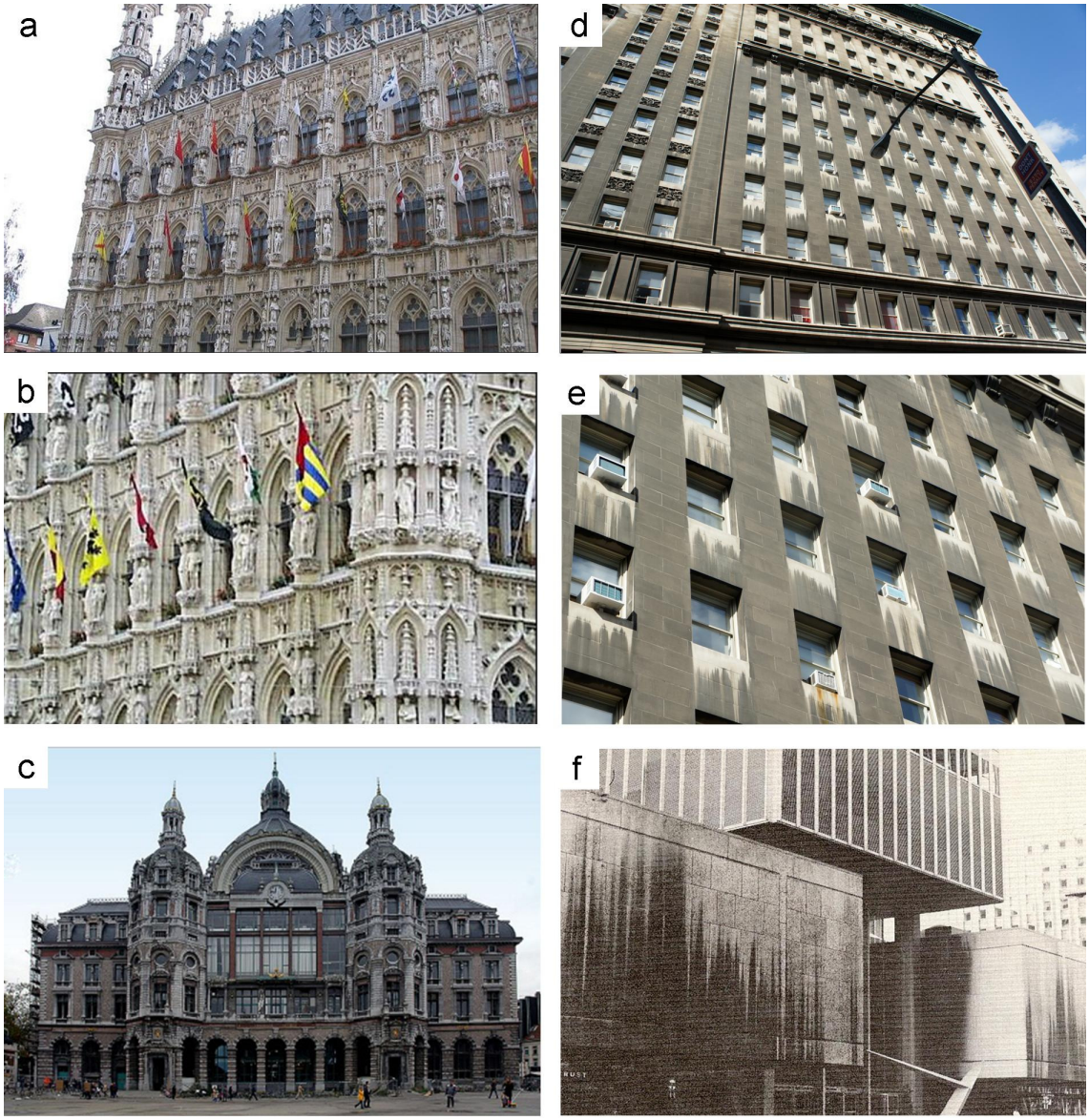

Figure 15. Surface soiling on historical and contemporary buildings: (a-b) City Hall, Leuven. (c) Central Railway Station, Antwerp. (d-f) Contemporary buildings with very visible soiling patterns. Dark colours indicate soiled areas, light colours indicate areas that have been cleaned by runoff (Fig. f from [189], reproduced with permission).

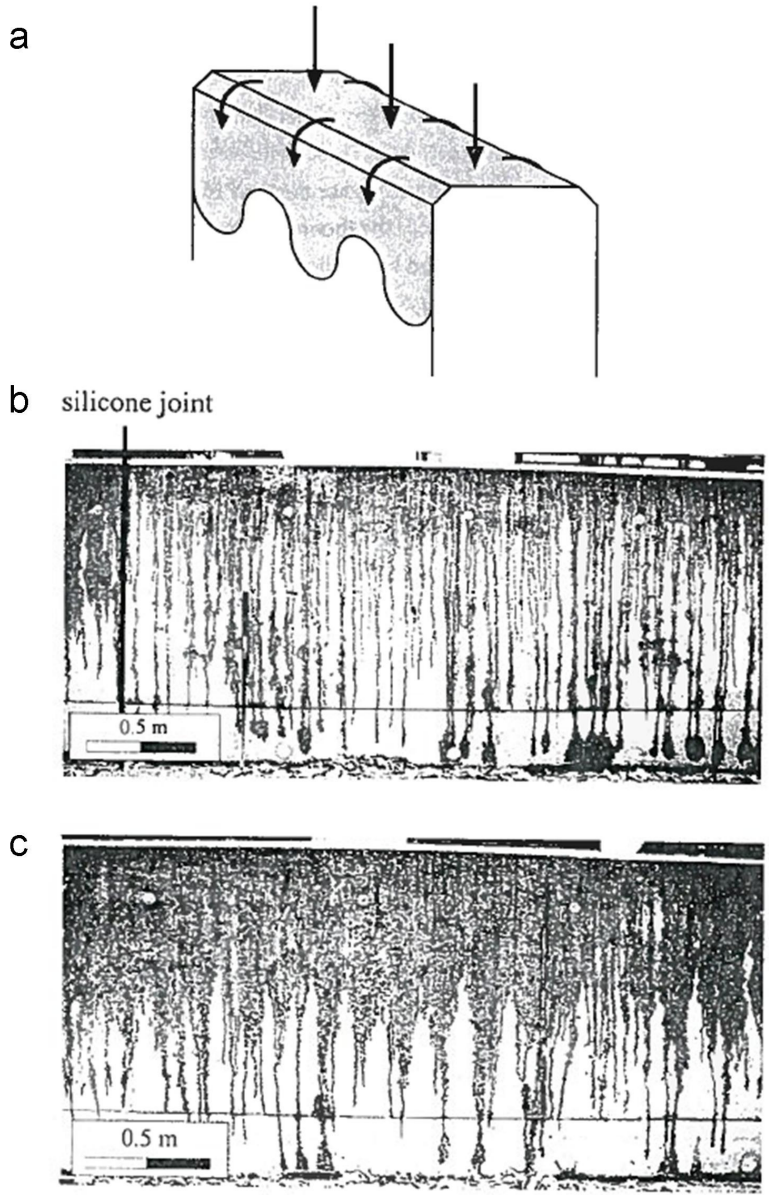

Figure 16. (a) Schematic representation of small vertical walls in study by Kuntz and van Mier [198]. (b-c) Wetting patterns with front instability ("fingers"): (b) less capillary action yielding long and narrow fingers; (c) more capillary action yielding shorter and wider fingers. The patterns correspond to wetting, not soiling. Dark colour indicates wetted areas and light colour indicates dry areas (from [198], reproduced with permission).

Figure 17. Gauges for measurement of wind-driven rain (plate-type gauge on the left) and runoff (collection gutter on the right) (from [200]).

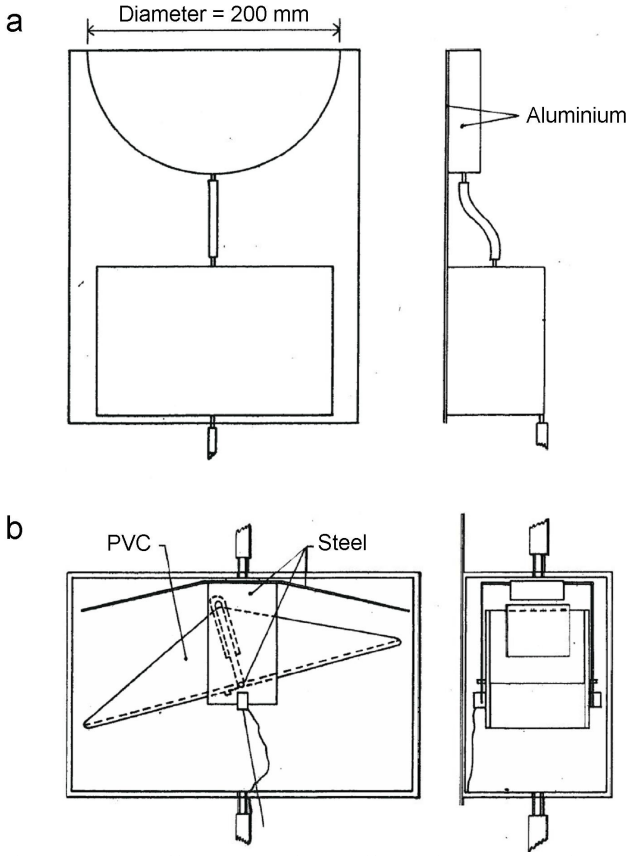

Figure 18. Runoff gauge used by Beijer and Johansson (from [39]).

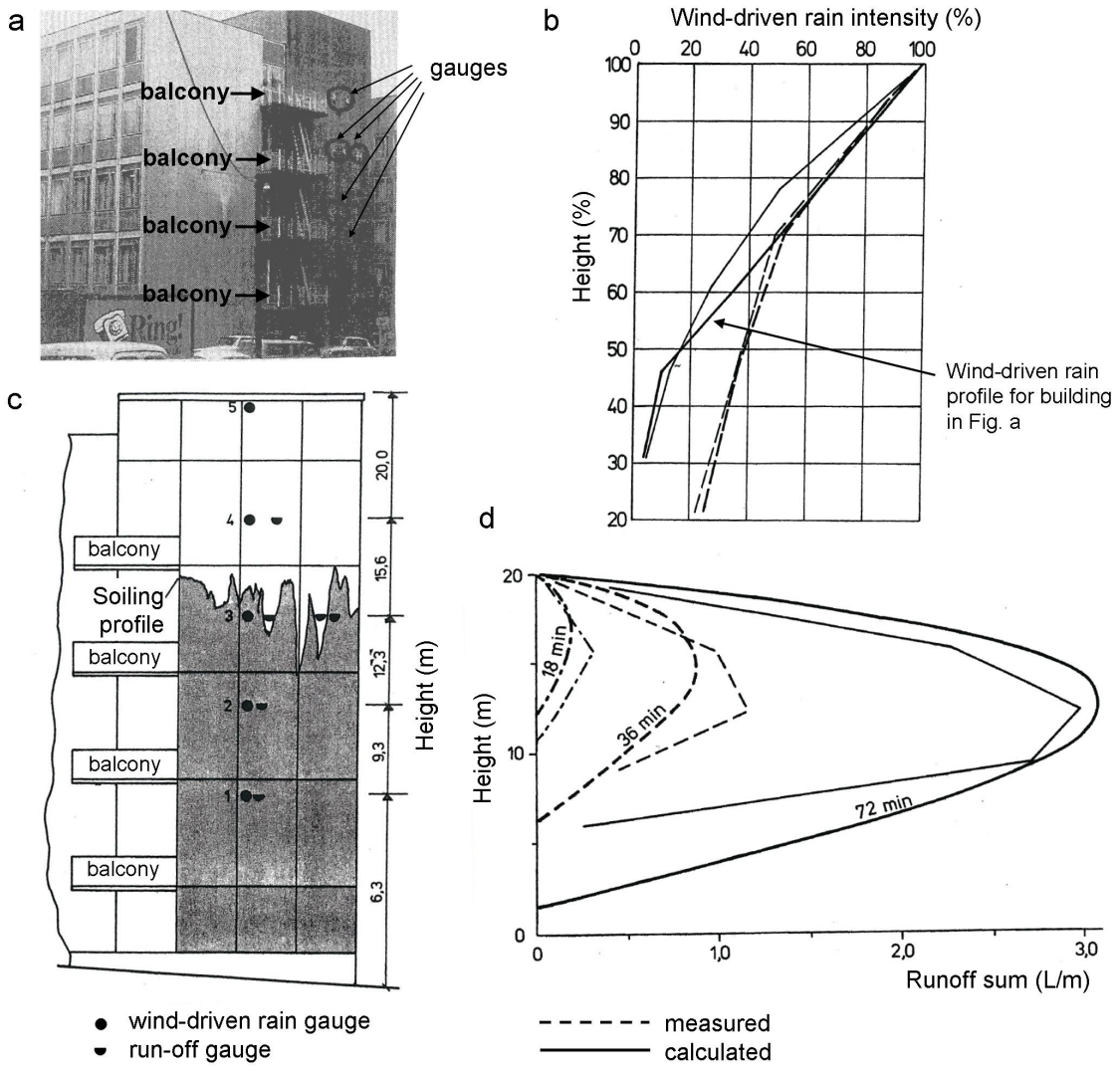

Figure 19. Measurements of wind-driven rain impingement and rainwater runoff by Beijer and Johansson (1976) on a concrete building facade in the Stockholm area [39]. (a) Photograph of building facade with indication of balconies and positions of gauges. (b) Measured wind-driven rain intensity profile at four buildings, including the building in Fig. a. (c) Schematic representation of building facade, surface soiling pattern and position of gauges. (d) Measured and calculated runoff sums on September 29, 1973, at 18, 36 and 72 min. after the start of the rain (from [39]).

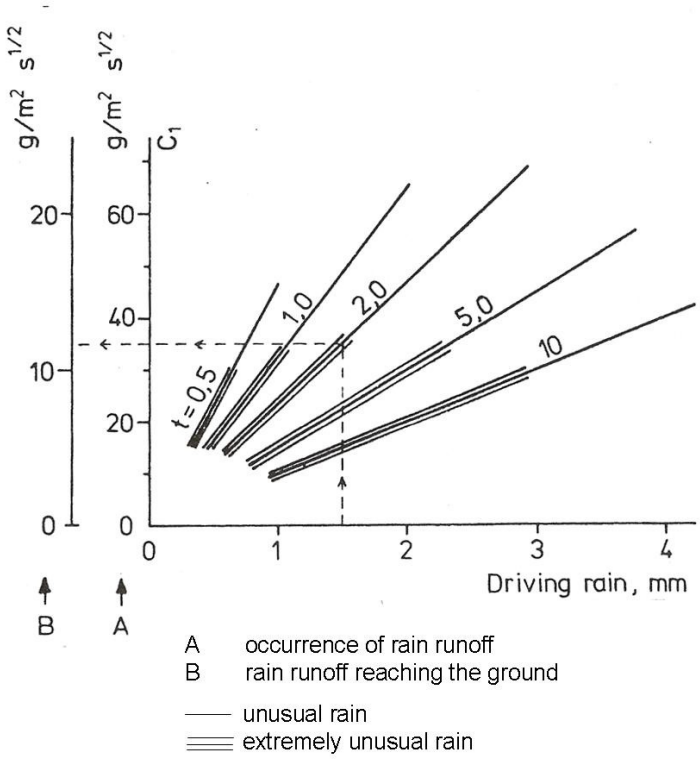

Figure 20. Diagram with maximum capillary water absorption coefficient C_1 for occurrence of rain runoff (A-axis) and for rain runoff reaching the ground (B-axis) for various wind-driven rain amounts and durations (t in hours) The single lines indicate the time after which A or B will take place during "unusual rain". The triple lines indicate the time after which A or B will occur during "extremely unusual rain" (from [40]).

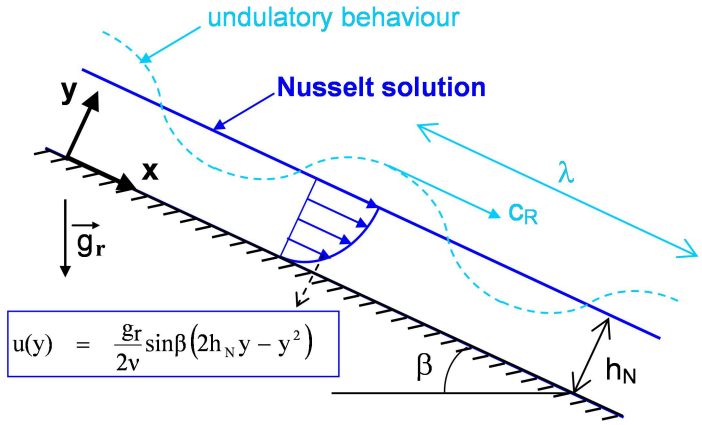

Figure 21: Schematic representation of thin film runoff down an inclined wall. Note: figure not to scale (from [50], reproduced with permission).

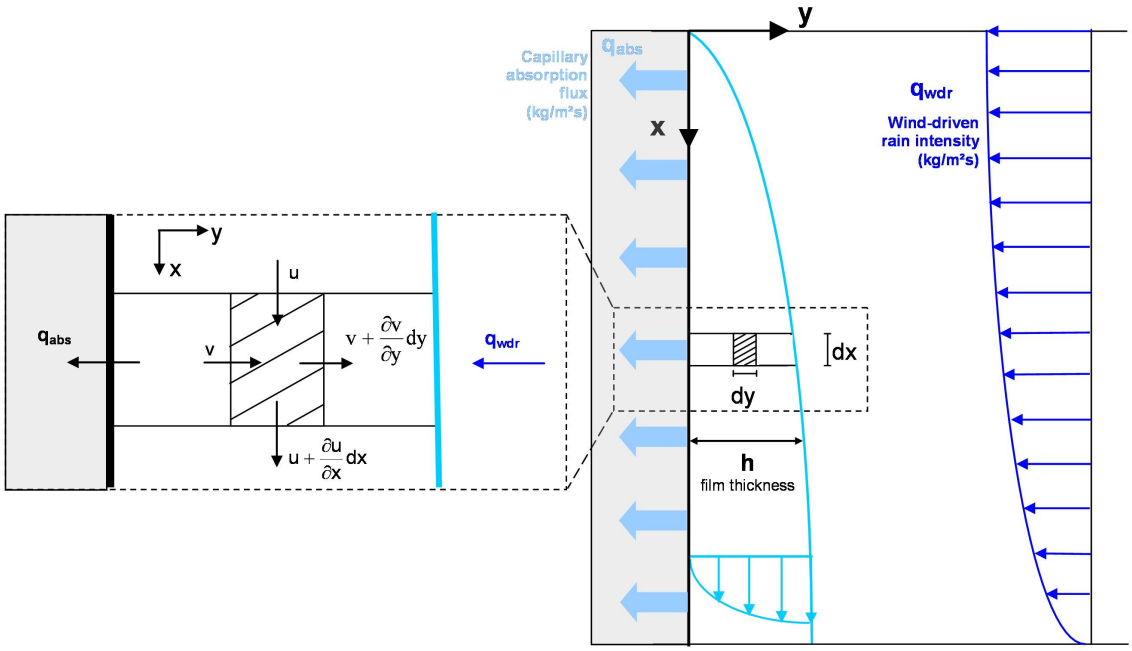

Figure 22. Schematic presentation and symbols for thin film runoff along a vertical wall with the wind-driven rain intensity and the capillary absorption flux as source and sink (from [50], reproduced with permission).

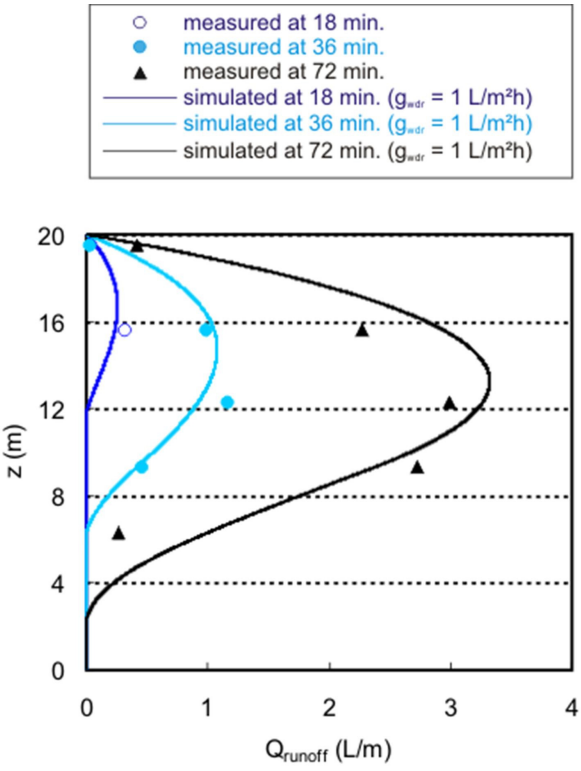

Figure 23. Comparison of numerical and experimental results for the runoff sum at 18, 36 and 72 minutes after the start of the rain (from [50], reproduced with permission).

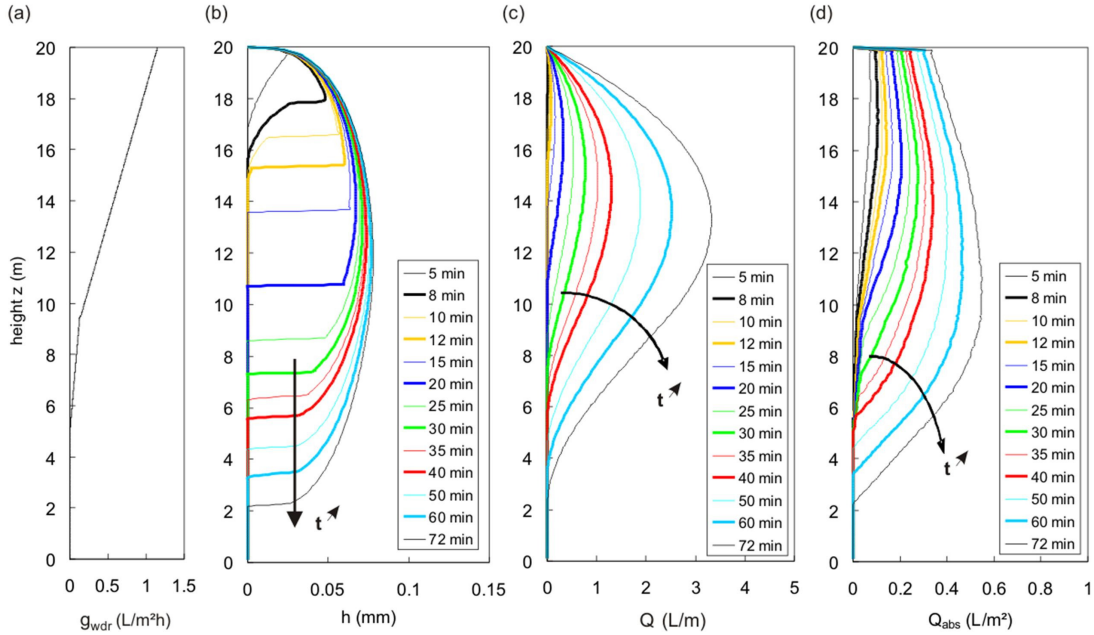

Figure 24. (a) Wind-driven rain intensity during the 72 min. rain event. (b-d) Corresponding numerical results for the 20 m high wall at different time steps for (b) film thickness; (c) runoff sum and (d) sum of absorbed water (from [50], reproduced with permission).